AN ABSTRACT OF THE THESIS OF

Garrett Holzwarth for the degree of Master of Science in Microbiology presented on February 27, 2018.

Title: Gadusol Production in *Saccharomyces cerevisiae*.

Abstract approved: _____

Alan T. Bakalinsky

Gadusol is a UV-B-absorbent compound found in fish and other marine organisms where it is presumed to play a role as a sunscreen and antioxidant. In light of commercial potential as a replacement for problematic synthetic sunscreens, a process to produce recombinant gadusol in the yeast *Saccharomcyces cerevisiae* was investigated. Gadusol is derived from the pentose phosphate pathway intermediate sedoheptulose 7-phosphate (S7P) in a two-step reaction catalyzed by 2-epi-5-epi-valiolone synthase (EEVS) and methyl transferase-oxidoreductase (MT-Ox). Zebrafish-derived *EEVS* and *MT-Ox* cDNAs were placed under the control of a constitutive yeast promoter on separate high-copy number plasmids and introduced into *S. cerevisiae* to generate strain G0 that produced about 12 mg/L. A number of genetic and cultural interventions were subsequently investigated in order to increase yields. Deletion of *TAL1* that encodes a well-characterized transaldolase catalyzing conversion of S7P and

glyceraldehyde 3-P to fructose 6-P and erythrose 4-P increased yields to 20 mg/L (G1). To assess the additive effect of deleting the less active of the two known yeast transaldolase genes (*NQM1*), strain G2 was constructed that lacked both *TAL1* and *NQM1* and which produced about 30 mg/L. Strain G3, the highest yielding strain, was constructed by replacing the two original EEVS and MT-Ox plasmids with a single construct containing both *EEVS* and *MT-Ox* genes integrated into a yeast chromosome. Gadusol levels reached about 64 mg/L in G3 which represents a 5-fold increase over G0. Various nutritional modifications of the G3 growth medium were not found to increase yields further. Similarly, interventions intended to force glycolytic intermediates towards S7P, namely overexpression of sedoheptulose 1,7-bisphosphatase and deletion of phosphoglucoisomerase did not increase yields.

Gadusol Production in *Saccharomyces cerevisiae*

by

Garrett Holzwarth

A THESIS

submitted to

Oregon State University

in partial fulfillment of
the requirements for the
degree of

Master of Science

Presented February 27, 2018
Commencement June 2018

Master of Science thesis of Garrett Holzwarth presented on February 27, 2018

APPROVED:

Major Professor, representing Microbiology

Head of the Department of Microbiology

Dean of the Graduate School

I understand that my thesis will become part of the permanent collection of Oregon State University libraries. My signature below authorizes release of my thesis to any reader upon request.

Garrett Holzwarth, Author

ACKNOWLEDGEMENTS

I would like to express my sincere gratitude to my advisor, Alan Bakalinsky, for his encouragement and patience throughout this project and the thesis writing process. I am deeply grateful to him for introducing me to the world of yeast genetics and all the possibilities it offers. Alan Bakalinsky is a co-founder and co-owner of Gadusol Laboratories, a company that intends to produce and sell gadusol-based sunscreen ingredients.

I would also like to thank my committee members Taifo Mahmud, Kim Halsey, and Andy Karplus for helpful discussions and taking the time to serve on my committee.

I am grateful for all of the lab mates and fellow scientist that have helped me with this project since the beginning. Specifically, Jun Ding, for helping me get started in the lab, Andrew Osborn for great discussions and Sam Bradford for his assistance with experiments. Undergraduates that have been an immense help to this work include Allen Yoshinaga, Van Ahn Vu, and E Seul Kim.

I would like to thank my parents for all of their love, support, and encouragement in pursuing my goals. I would also like to express my gratitude to my girlfriend, Andrea, and all of my friends in the microbiology graduate school.

CONTRIBUTION OF AUTHORS

Garrett Holzwarth performed experiments, analysis, and wrote the thesis draft. Dr. Alan Bakalinsky was the primary investigator for this project and was involved in experimental design and the writing of the thesis. Dr. Taifo Mahmud provided EEVS and MTOx cDNAs, and HPLC-MS data confirming production of gadusol by *Saccharomyces cerevisiae*. C. Samuel Bradford assisted with construction of several yeast strains.

TABLE OF CONTENTS

TABLE OF CONTENTS (Continued)

Page

LIST OF FIGURES

LIST OF FIGURES (Continued)

LIST OF TABLES

1 Introduction

1.1 Gadusol

1.1.1 Discovery of Gadusol

Gadusol (Fig. 1) was first identified in the early 1980's by workers at the National Environmental Research Council, Institute of Marine Biochemistry based in Scotland. The team was investigating the composition of roe in fish off the coast of Aberdeen. Gadusol was initially found in the roe of *Gadus morhua* where its UV-absorbent properties were identified (Grant 1980). Subsequently, it was observed in the roe of several additional fish species (*Melanogrammus aeglefinus*, *Limanda platessa, Hippoglossoides platessa, Platichthys flesus, Pleuronectes platessa,* and *Microstomus kitt*) and in sea urchin eggs (Plack et al. 1981; Chioccara et al. 1986). Plack et al. (1981) reported 4.3±0.30 (mg/g dry wt.) in the roe and between 0.10 to 0.01 mg/g dry wt. gadusol in the tissue of *G. morhua*. The higher levels observed in ovaries suggested that gadusol played a protective role in fish roe. Similar levels were reported for the other fish species studied (Plack et al. 1981).

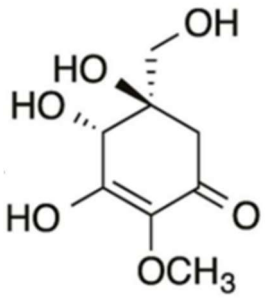

Figure 1. Gadusol.

1.1.2 Chemical properties

Gadusol or 3,5,6-trihydroxy-5-hydroxymethyl-2-methoxycyclohex-2-en-1-one is a cyclohexanone tautomer. Gadusol shifts between enol and enolate forms as a function of pH as shown in Fig. 2. The enol (gadusol) form dominates at lower pH and has a λ_{max} of 269 nm, while at neutral and basic pH the enolate (gadusolate) form dominates with a λ_{max} of 296 nm (Plack et al. 1981). Gadusolate is the more effective sunscreen with an

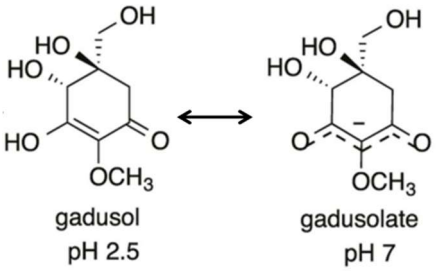

Figure 2. pH-dependent tautomers of gadusol, adapted from (Osborn et al. 2015).

extinction coefficient of 21,800 M^{-1} cm^{-1} compared to 12,400 M^{-1} cm^{-1} for gadusol (Arbeloa et al. 2011). The gadusolate form absorbs light in the UV-B region (290-315 nm). Estimating how much UV-B light penetrates the Earth's atmosphere is difficult because many factors affect UV absorbance. Two major factors include solar angle and the presence of UV-absorbent compounds. The combination of these factors makes it difficult to estimate a typical UV-B dose or how far UV light penetrates into bodies of water (Booth and Morrow 1997). Gadusolate is more photostable than gadusol. Arbeloa et al. (2011) investigated the photodecomposition of gadusol and gadusolate by monitoring the change in gadusol concentration as a function of UV-light absorbed at their respective absorbance maxima. They found that gadusolate, the form that predominates at physiological pH, has a quantum yield of photodecomposition 260 times greater than gadusol indicating that gadusolate can absorb a larger quantity of light before breaking down (Arbeloa et al. 2011). Throughout the remainder of this thesis, "gadusol" will be used generically to refer to both tautomers, unless a distinction is needed for clarity.

Arbeloa et al. (2010) measured gadusol's antioxidant properties using an oxygen radical absorption capacity assay (ORAC) and a radical scavenging assay with 2,2'-azinobis(3- ethylbenzothiazoline-6-sulphonic acid) diammonium salt (ABTS). In the ORAC assay, gadusol exhibited 6-times the activity reported for ascorbic acid. However, by the ABTS decolorization assay, gadusol was found to have an antioxidant capacity comparable to that of ascorbic acid (Arbeloa et al. 2010).

1.1.3 Biosynthesis

Gadusol is synthesized from sedoheptulose 7-P (S7P), a pentose phosphate pathway (PPP) intermediate. As shown in Fig. 3, 2-*epi*-*5*-epi-valiolone synthetase (EEVS) initially cyclizes S7P to 2-*epi*-5-*epi*-valiolone (EEV). A bifunctional methyltransferase-oxidase (MT-Ox) then catalyzes the S-adenosyl methionine (SAM)-dependent methylation and NAD^+-dependent oxidation of EEV to gadusol (Fig. 3).

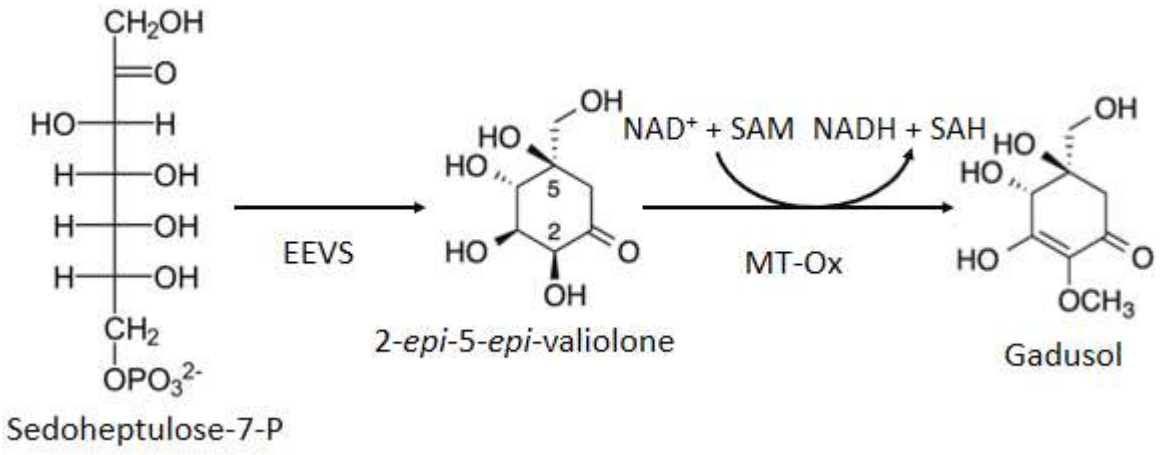

Figure 3. Biosynthesis of gadusol.

1.1.4 Function

While chemical data for gadusol suggest a role as a sunscreen and antioxidant, *in vivo* studies are less clear. Gadusol's high molar absorptivity in the UV-B range first led to suggestions for a role as a sunscreen (Plack et al. 1981). Sunscreens like gadusol protect tissues by absorbing UV light before it can damage cells. UV-B causes damage

through at least two known mechanisms. It induces pyrimidine dimer formation in DNA, leading to mutations and can also generate free radicals which lead to oxidation of lipids and proteins (Sinha and Häder 2002). The photostability of the gadusolate tautomer found at physiological pH supports a sunscreen role (Arbeloa et al. 2011). However, gadusol is found in relatively low concentrations in fish tissues except in the roe (Plack et al. 1981). It is unclear if fish eggs are routinely exposed to enough sunlight to require UV-B protection. With respect to microbes, Gao and Garcia-Pichel (2011) have argued that as cell size decreases, the amount of sunscreen required to provide protection increases significantly. In order for a sunscreen to be effective, it must be sufficiently concentrated to prevent UV irradiation from penetrating the periphery of the cell and reaching molecular targets. Sunscreens like gadusol, which are soluble in the cytosol, must reach a high-intracellular concentration to provide such protection (Garcia-Pichel 1994; Gao and Garcia-Pichel 2011). While gadusol has also been shown to exhibit antioxidant activity *in vitro*, it is not clear to what extent it contributes to such activity *in vivo* where NADPH and GSH play prominent roles. To my knowledge, experiments demonstrating gadusol's antioxidant properties *in vivo* have not been performed. Gadusol may also have protective and tuning roles in animal vision, as it has been found in the lenses of the eyes of several marine animals. In addition to protecting sensitive tissues from UV-B-damage (Dunlap et al. 1989), gadusol also helps tune the UV vision of mantis shrimp by absorbing light in the 296-nm range, preventing activation of receptors that absorb light at that wavelength (Bok et al. 2014).

The origins of gadusol biosynthesis are unclear, but one theory proposes an origin in cyanobacteria, prior to the formation of an oxygen-containing atmosphere on Earth. At

such a time, the Earth's surface was exposed to much higher levels of solar-UV irradiation. Elevated levels of UV irradiation likely selected for the evolution of UV-protective compounds, particularly in organisms such as cyanobacteria, which are dependent on photosynthesis as a source of energy (Garcia-Pichel 1998). However, once oxygen became a significant component in the atmosphere, the amount of UV light reaching the surface dropped dramatically. After evolving in bacteria, EEVS and MT-Ox are thought to have undergone horizontal (non-sexual) transfer to eukaryotes. This transfer led to the presence of EEVS and MT-Ox genes in fish, amphibians, reptiles, birds, and stramenopiles (Osborn et al. 2015). In Earth's current oxygen-containing atmosphere, most solar UV-C (100-280 nm) is absorbed by atmospheric ozone. While some UV-B (280-315 nm) is absorbed by the ozone layer, a significant amount reaches the Earth's surface. UV-A (315-400 nm) irradiation is only slightly attenuated by the atmosphere (Gao and Garcia-Pichel 2011).

1.2 Biochemistry relevant to gadusol production in yeast

1.2.1 Sedoheptulose 7-P

Sedoheptulose 7-P (S7P) is the natural precursor of gadusol and is a central intermediate in the pentose phosphate pathway, but is also derived from glycolytic intermediates (Fig. 4). In yeast, most glucose is metabolized by glycolysis, however, it has been estimated that about 20% is metabolized by the oxidative pentose phosphate pathway to generate reducing equivalents (NADPH) and pentoses to meet biosynthetic needs, depending on growth conditions and genotype (Van Winden et al. 2005; Cadière et al. 2011). NADPH is primarily consumed in the biosynthesis of fatty acids, sulfur-

containing amino acids, and deoxynucleotides (Stincone et al. 2015). NADPH is also produced to help counteract oxidative stress by serving as a cofactor in the glutathione reductase-dependent regeneration of glutathione from glutathione disulfide (Stincone et al. 2015). The pentose phosphate pathway is largely regulated by altering flux through the rate-limiting step, glucose-6-phosphate dehydrogenase (*ZWF1*), at both protein and transcriptional levels (Stincone et al. 2015).

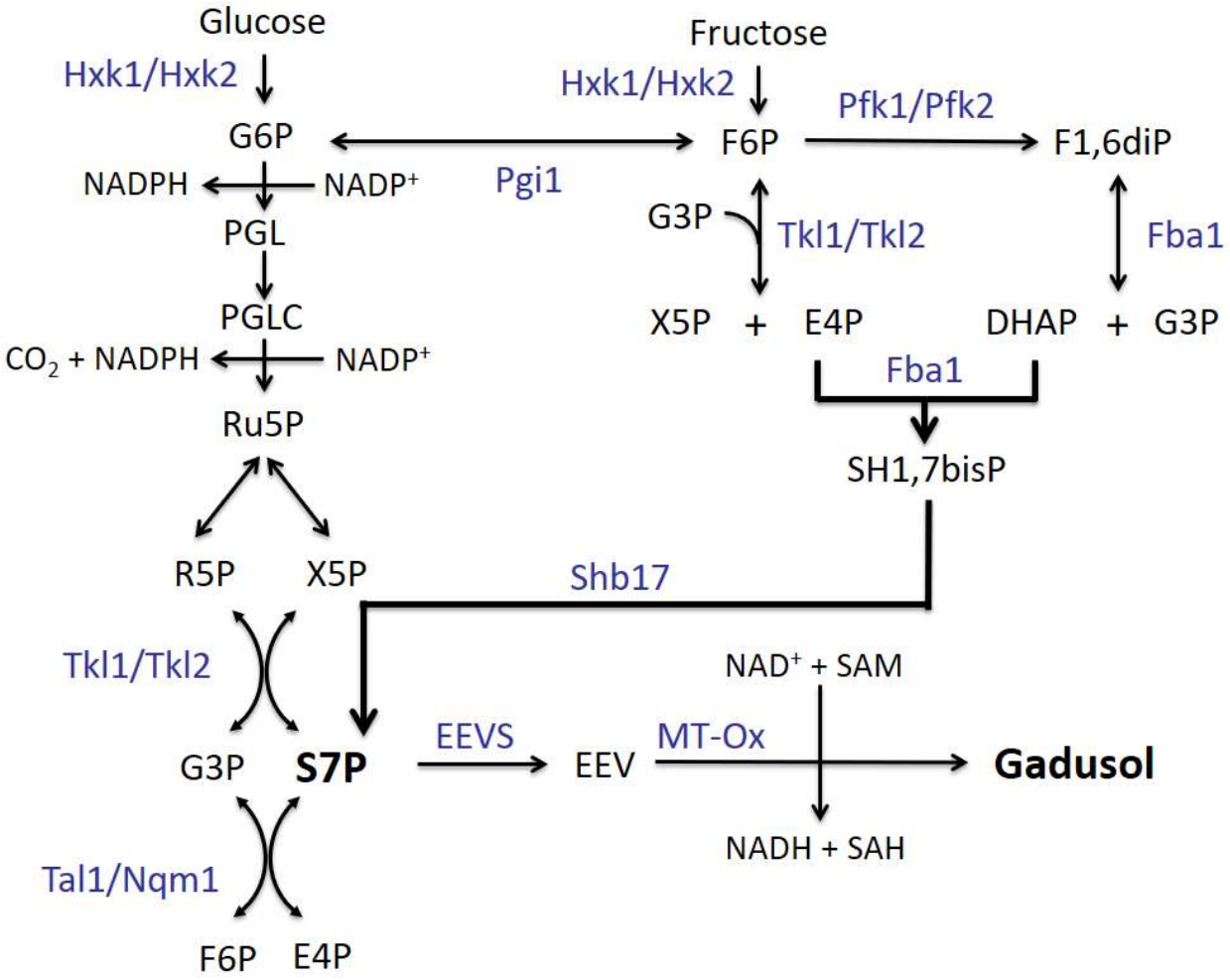

Figure 4. Pathways related to gadusol biosynthesis. Enzymes are labeled in blue and intermediates are labeled in black. Abbreviations: DHAP, dihydroxyacetone phosphate; E4P, erythrose 4-P; EEVS, 2-*epi*-5-*epi*-valiolone synthetase; F1,6diP, fructose 1,6-P; F6P, fructose 6-P; Fba1, Fructose bisphosphate aldolase; G3P, glyceraldehyde 3-P; G6P, glucose 6-P; Hxk1/2, Hexokinase; MT-Ox, Methyl transferase oxidase; Pfk1/2, phosphofructokinase; Pgi1, Phosphoglucoisomerase; PGL, phosphogluconolactone; PGLC, phosphogluconate; Ru5P, ribulose 5-P; R5P, ribose 5-P; Shb17, Sedoheptulose 1,7-bisphosphatase; S7P, sedoheptulose 7-P; and and SH1,7bisP, sedoheptulose 1,7-P

Tal1/Nqm1, Transaldolase; Tkl1/Tkl2, Transketolase; and X5P, xylulose 5-P. Gadusol and its precursor S7P are shown in bold.

1.2.2 Pentose phosphate pathway

The oxidative phase of the pentose phosphate pathway (PPP) is composed of three steps that generate two NADPH, a CO_2 and the S7P precursor, ribulose 5-phosphate. For emphasis, the oxidative phase of the pentose phosphate pathway originally shown in Fig. 4 is in indicated by a red dashed box in Fig. 5. The pathway begins with an irreversible step that oxidizes glucose 6-P (G6P) to phosphogluconolactone (PGL) while reducing $NADP^+$ to NADPH. PGL is then oxidized to phosphogluconate, yielding another NADPH, CO_2 and ribulose 5-P (Ru5P).

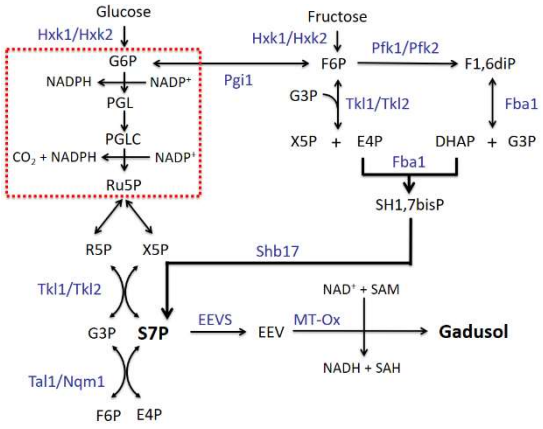

Figure 5. The oxidative phase of the PPP (red dashed box) in relation to gadusol biosynthesis.

The non-oxidative phase of the pentose phosphate pathway shuffles carbons between intermediates to generate a variety of phosphosugars, including S7P, the precursor for gadusol. The non-oxidative phase of the pentose phosphate pathway originally shown in Fig. 4 is indicated by the red dashed box in Fig. 6. The transketolase step encoded by *TKL1* and *TKL2* reversibly

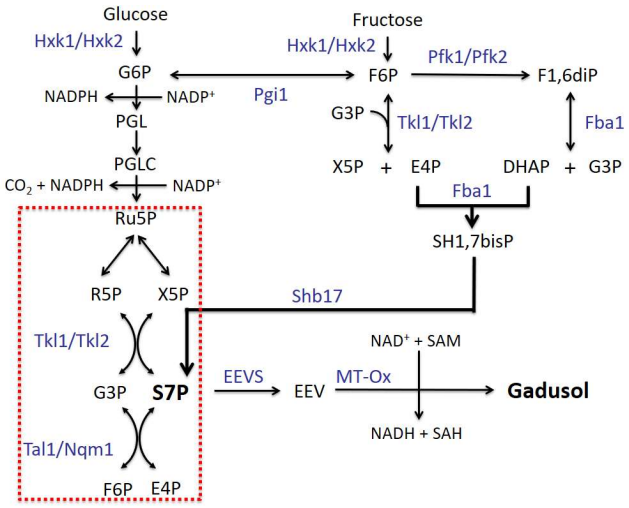

Figure 6. The non-oxidative phase of the PPP (red dashed box) in relation to gadusol biosynthesis.

generates S7P and glyceraldehyde 3-P (G3P) from the PPP intermediates ribose 5-P (R5P) and xylulose 5-P (X5P) (Schaaff et al. 1990). The S7P precursor, sedoheptulose 1,7-bisphosphate (SH1,7bisP) can also be generated through an alternative activity of fructose bisphosphate aldolase (Fba1) acting on the PPP intermediate erythrose 4-P and the glycolytic intermediate dihydroxyacetone phosphate (DHAP) (Clasquin et al. 2011). SH1,7bisP can then be dephosphorylated to yield S7P by the phosphatase Shb17. Transaldolase reversibly converts S7P and glyceraldehyde 3-P into fructose 6-P and erythrose 4-P. Two yeast-transaldolase paralogs exist, *TAL1* and *NQM1*. Tal1 is the active transaldolase in cells grown on glucose. *tal1Δ* mutants lack transaldolase activity when incubated on glucose because *NQM1* is not expressed when cells grow on fermentable substrates (Huang et al. 2008; Michel et al. 2015). *tal1Δ* mutants also accumulate S7P, as noted in a report of a >30-fold increase relative to a wild-type strain grown on glucose (Schaaff et al. 1990). *tal1Δ* mutants have also been observed to be more sensitive to oxidative stress (Ng et al. 2008). Accumulation of S7P and other pentose phosphates could inhibit flux through the oxidative portion of the pentose phosphate pathway, depriving cells of the NADPH needed to regenerate glutathione.

1.2.3 Sedoheptulose 7-P biosynthesis via glycolytic intermediates

An alternative S7P biosynthetic pathway was recently described based on a previously unknown activity of Fba1 described above, and a newly-discovered phosphatase, Shb17 (Clasquin et al. 2011). This pathway originally shown in Fig. 4 is indicated by the red dashed box in Fig. 7. Previously,

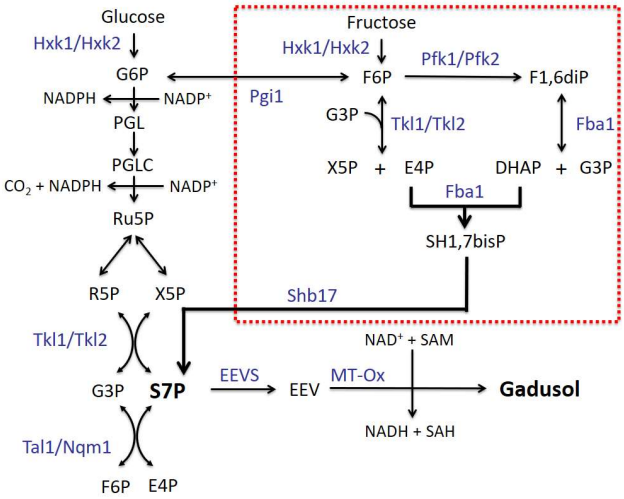

Figure 7. S7P biosynthesis (red dashed box) from glycolytic intermediates in relation to gadusol.

Fba1 was only thought to catalyze the conversion of fructose 1,6-P to dihydroxyacetone-P (DHAP) and glyceraldehyde 3-P. Recently, an additional activity was discovered, the reversible conversion of erythrose 4-P and DHAP into sedoheptulose 1,7-P. This previously unrecognized activity was confirmed through labeling experiments where ^{13}C-labeled DHAP and erythrose 4-P led to the production of doubly-labeled sedoheptulose 1,7-P (SH1,7bisP) (Clasquin et al. 2011). Shb17, a bisphosphatase, dephosphorylates SH1,7bisP to sedepheptulose 7-P. Clasquin et al. (2011) hypothesized that this shunt pathway provided carbon from glycolysis to produce ribose 5-P when NADPH was not required. To support this hypothesis, the authors monitored Shb17 activity under conditions leading to high- and low-NADPH demand. They found that supplementing the growth medium with lipids and aromatic amino acids that presumably reduced demand for NADPH, led to a two-fold increase in flux through Shb17 (Clasquin et al. 2011).

The combined deletion of *TAL1* and *PGI1* was reported to increase accumulation of S7P 4-fold, relative to a *tal1* mutant (Schaaff et al. 1990). Phosphoglucoisomerase (*PGI1*) catalyzes the isomerization of glucose 6-P to fructose 6-P. One characteristic of *pgi1Δ* mutants is an inability to grow on glucose as sole carbon source (Aguilera 1987; Schaaff et al. 1990). Schaaff et al. (1990) isolated *pgi1Δ* mutants on growth medium containing 2% fructose and 0.1% glucose. *pgi1Δ* mutants must rely on the S7P shunt or Tal1 activity to generate ribose 5-P for growth because they cannot generate glucose 6-P from fructose. *tal1 pgi1* double mutants are forced to route carbon exclusively through the *SHB17*-shunt pathway to meet the cell's need for ribose 5-P. Because *pgi1* mutants are also unable to generate NADPH via the oxidative portion of the pentose phosphate pathway, they oxidize more acetaldehyde via an $NADP^+$-dependent cytosolic aldehyde dehydrogenase (*ALD6*) and/or oxidize more isocitrate via $NADP^+$-dependent cytosolic isocitrate dehydrogenase (*IDP2*) (Grabowska and Chelstowska 2003; Minard and McAlister-Henn 2005). Although *pgi1Δ* mutants cannot grow on glucose, a small amount (0.1%) is required for growth on fructose (Aguilera 1987). This requirement may arise from the role of glucose as a signaling molecule needed to induce expression of ribosomal protein genes (Pernambuco et al. 1996).

The preceding discussion about formation of S7P in *S. cerevisiae* provides context for production of gadusol in yeast because S7P is the key precursor. From a commercial perspective, obtaining gadusol from the marine organisms in which it is produced naturally is unsustainable for at least two reasons. First, the concentration of gadusol in these organisms is likely to be low, limited by physiologic need. Second,

harvesting and extracting gadusol from environmental sources could endanger fragile ecosystems and likely would require environmental impact studies to assess the risks. Expressing the biosynthetic genes in yeast provides an opportunity to leverage in-depth knowledge of yeast biochemistry to generate a sustainable process. Similar processes have been developed for several therapeutics or their precursors including artemisinic acid and opioids. Supplies of artemisinin, an antimalarial drug, are limited by the scarcity of the plant *Artemisia annua*. Researchers at the University of California, Berkeley have engineered a strain of *S. cerevisiae* to produce the precursor artemisinic acid, permitting cheaper production of semisynthetic artemisinin (Ro et al. 2006). Manufacture of analgesic opioids is dependent on stable sources of the compounds. However, the opium poppy *Papaver somniferum* is sensitive to climatic conditions and diseases which can lead to shortages. To address these problems, workers at Stanford University have developed yeast strains that produce several opioid compounds, codeine, morphine, hydromorphone, hydrocodone, and oxycodone (Thodey et al. 2014).

2 Materials and Methods

2.1 Media and growth conditions

Cells were grown in 2X YEPD (2% yeast extract, 4% peptone, and 4% glucose) for transformations, and in minimal medium (M) (Bacto yeast nitrogen base [YNB] without amino acids) (6.7 g/L) + 2% glucose supplemented with histidine (20 μg/ml), leucine (30 μg/ml), lysine (30 μg/ml), tryptophan (20 μg/ml), or uracil (10 μg/ml) as needed. *pgi1* mutants were grown in YNB + 2% fructose + 0.1% glucose with supplements as needed. “YNB+NADPH nutr.” is YNB + 2% glucose supplemented with 20 μg/ml ergosterol from a 2 mg/ml ergosterol stock dissolved in 1:1 (vol/vol) EtOH:Tween 80, lysine (30 μg/ml), tryptophan (20 μg/ml), histidine (20 μg/ml), phenylalanine (50 μg/ml), and tyrosine (30 μg/ml). Stocks of all antibiotics were stored at -20°C. Ampicillin was prepared as an aqueous sterile-filtered 1000X stock (100 mg/ml). G-418 was prepared as an aqueous sterile-filtered 500X stock (100 mg/ml). Hygromycin B was prepared as an aqueous sterile-filtered 500X stock (150 mg/ml). The stocks were filtered through a sterile 0.45-μm filter. Agar-based media were sterilized by autoclaving. Liquid cultures were grown at 30°C and 200 rpm; plates were incubated statically at 30°C.

For growth and gadusol experiments, isolated colonies from selective media were used to inoculate 2 ml cultures. The 2 ml cultures were grown for either 16 or 48 h at 30°C and 200 RPM. Cells were harvested by centrifugation, washed with sterile water, and counted using hemocytometer. Cells were inoculated into 75 ml of media that was then split into three 25 ml cultures in 125-ml Erlenmeyer flasks to yield an initial

cell density = 10^5 cell/ml. Cultures were incubated at 30°C and 200 RPM. Cultures were sampled periodically to measure growth (A_{600}) and gadusol (A_{296}).

2.2 Transformations

Yeast was transformed using the lithium acetate method (Gietz and Woods 2001). Briefly, the strain to be transformed was grown overnight at 30ºC and 200 RPM in 1 ml of 2XYEPD in an incubator shaker. The overnight culture was used to inoculate 25 ml of 2XYEPD at a concentration of $5X10^6$ cells/ml. The 25 ml 2XYEPD culture was kept at 30ºC and 200 RPM until at least two cell doublings had occurred. Cells were then harvested by centrifugation at 1,200 *g* and washed twice with sterile water. An aliquot of $2X10^8$ cells was then transferred to a 1.5 ml Eppendorf tube and centrifuged at 16,000 RPM in a microcentrifuge. Supernatant was removed from the tube without disturbing cells. The following chemicals and DNAs were then added in this specific order: 240 µl 50% (w/v) polyethylene glycol 3500, 36 µl lithium acetate, 50 µl 2.0 mg/ml single-stranded carrier DNA, and 34 µl of plasmid or PCR amplicon DNA. The transformation mixture was then mixed by pipetting and incubated at 42ºC for 40 minutes. Cells were pelleted to remove the transformation mixture and then washed with 1 ml of sterile water before plating on selective media.

E. coli strains were transformed according to suppliers' directions for chemically competent TOP10 cells (Invitrogen) and NEB-2β cells (New England Biolabs). Suppliers' directions briefly stated that 50 µl aliquots of the cells were to be removed from -70ºC storage and thawed on ice for 10 minutes. A 1-5 µl aliquot of DNA was

added to the thawed cells followed by a 30-minute incubation on ice. After the incubation, the DNA-treated cells were heat shocked for 30 sec at 42ºC followed by a second 5 min incubation on ice. Cells were resuspended in 950 µl of SOC medium before aliquots were plated on selective media and grown at 37ºC.

2.3 Strain construction

E. coli strains (Table 1) maintained on LB+amp at 37ºC. Liquid cultures were grown at 37ºC and shaken at 200 RPM.

Table 1. *E. coli* strains

Strain	**Genotype**	**Origin**
BL21	B F$^-$ *ompT gal dcm lon hsdS$_B$*($r_B^- m_B^-$) [*malB*$^+$]$_{K\text{-}12}$(λ^S)	Stratagene Inc., CA
DH5α	F$^-$ *endA1 glnV44 thi-1 recA1 relA1 gyrA96 deoR nupG purB20* φ80d*lacZ*ΔM15 Δ(*lacZYA-argF*)U169, hsdR17($r_K^- m_K^+$), λ$^-$	ThermoFisher Scientific Inc., Waltham, MA
NEB-5α	DH5α derivative	New England Biolabs Inc., Ipswich, MA
NEB-10β	DH10B derivative, F– *mcr*A Δ(*mrr-hsd*RMS-*mcr*BC) Φ80*lac*ZΔM15 Δ*lac*X74 *rec*A1 *end*A1 *ara*D139 Δ(*ara leu*) 7697 *gal*U *gal*K *rps*L *nup*G λ–	New England Biolabs Inc., Ipswich, MA
TOP10	F- *mcrA* Δ(*mrr-hsd*RMS-*mcr*BC) Φ80*lac*ZΔM15 Δ *lac*X74 *rec*A1 *ara*D139 Δ(*araleu*)7697 *gal*U *gal*K *rps*L (StrR) *end*A1 *nup*G	ThermoFisher Scientific Inc., Waltham, MA

Yeast strains (Table 2) were constructed as described below.

Table 2. Yeast strains.

Strain	**Genotype**	**Origin**
BY4742	MATα *his3Δ1 leu2Δ0 lys2Δ0 ura3Δ0*	ATC 204508, Manassas,VA
BY4742 *tal1Δ*	MATα *tal1Δ::KanMX4 his3Δ1 leu2Δ0 lys2Δ0 ura3Δ0*	Thermo Fisher Scientific Inc., Waltham, MA
BY4742 *trp1Δ*	MATα *his3Δ1 leu2Δ0 lys2Δ0 ura3Δ0 trp1Δ::URA3*	This study
G0	MATα *his3Δ1 leu2Δ0 lys2Δ0 ura3Δ0 trp1Δ::URA3*/pXP416-MTOx, pXP420-EEVS	This study
G1	MATα *tal1Δ::KanMX4 his3Δ1 leu2Δ0 lys2Δ0 ura3Δ0 trp1Δ::URA3*/pXP416-MTOx, pXP420-EEVS	This study
G2	MATα *tal1Δ::KanMX4 nqm1Δ::LEU2 his3Δ1 leu2Δ0 lys2Δ0 ura3Δ0 trp1Δ::URA3*/pXP416-MT-Ox, pXP420-EEVS	This study
G2C	MATα *tal1Δ::KanMX4 nqm1Δ::LEU2 his3Δ1 leu2Δ0 lys2Δ0 ura3Δ0 trp1Δ::URA3*/pXP416, pXP420	This study
G3	MATα *tal1Δ::KanMX4 nqm1Δ::LEU2 his3Δ1::pGH420-EEVS-MTOx-2μΔ leu2Δ0 lys2Δ0 ura3Δ0 trp1Δ::URA3*	This study
G4	MATα *tal1Δ::KanMX4 nqm1Δ::LEU2 pgi1Δ::TRP1 his3Δ1::pGH420-EEVS-MTOx-2μΔ leu2Δ0 lys2Δ0 ura3Δ0 trp1Δ::URA3*	This study
G5	MATα *tal1Δ::KanMX4 pgi1Δ::TRP1 his3Δ1::pGH420-EEVS-MTOx-2μΔ leu2Δ0 lys2Δ0 ura3Δ0 trp1Δ::URA3*	This study
G6	MATα *tal1Δ::KanMX4 nqm1Δ::Leu2 shb17Δ::HphMX his3Δ1 leu2Δ0 lys2Δ0 ura3Δ0 trp1Δ::URA3*/pXP416-MTOx, pXP420-EEVS	This study
G7	MATα *tal1Δ::KanMX4 nqm1Δ::Leu2 his3Δ1::pGH420-EEVS-MTOx-2μΔ leu2Δ0 lys2Δ0 ura3Δ0 trp1Δ::URA3/* pXP416-*SHB17*	This study
G8	MATα *tal1Δ::KanMX4 nqm1Δ::Leu2 his3Δ1::pGH420-EEVS-MTOx-2μΔ TEF1 TEF1::*pXP416-*SHB17-2μΔ leu2Δ0 lys2Δ0 ura3Δ0 trp1Δ::URA3*	This study
G9	MATα *tal1Δ::KanMX4 his3Δ1 leu2Δ0 lys2Δ0 ura3Δ0 pho13Δ*::*HphMX trp1Δ::URA3*/pXP416-MT-Ox, pXP420-EEVS	This study
G10	MATα *tal1Δ::KanMX4 his3Δ1 leu2Δ0 lys2Δ0 ura3Δ0 trp1Δ::URA3*/pXP416-MT-Ox, pXP420-EEVS, pXP422-*ZWF1*	This study

2.3.1 G0 (BY4742 *trp1*/pXP416-MTOx, pXP420-EEVS)

TRP1 in BY4742 was deleted by replacement with a 1.8 Kb PCR amplicon encoding *URA3*. The *URA3* amplicon was generated using the TRP1DisURA3UP/LO primers according to standard methods (Baudin et al. 1993; Gietz and Woods 2001). Transformants were selected on M+his+trp+leu+lys. The deletion of *TRP1* was confirmed by diagnostic PCR, using the TRP1DisUP/LO primers to generate a unique PCR amplicon of the *URA3* gene inserted at the *TRP1* locus (1.9 Kb). The BY4742 *trp1Δ* strain was co-transformed with both pXP416-MTOx and pXP420-EEVS using the lithium acetate method (Gietz and Woods 2001). Transformants were selected and maintained on M+leu+lys.

2.3.2 G1 (BY4742 *tal1Δ trp1Δ*/pXP416-MTOx, pXP420-EEVS)

TRP1 in BY4742 *tal1Δ::KanMX4* was deleted by replacement with a 1.8 Kb PCR amplicon encoding *URA3*. The *URA3* amplicon was generated using the TRP1DisURA3UP/LO primers according to standard methods (Baudin et al. 1993; Gietz and Woods 2001). Transformants were selected on M+his+trp+leu+lys+G418. Deletion of *TRP1* was confirmed by diagnostic PCR using the TRP1DisUP/LO primers to generate a unique PCR amplicon of the *URA3* gene inserted at the *TRP1* locus (1.9 Kb). The BY4742 *tal1Δ trp1Δ* strain was co-transformed with both pXP416-MTOx and pXP420-EEVS using the lithium acetate method (Gietz and Woods 2001). Transformants were selected and maintained on M+leu+lys.

2.3.3 G2 (BY4742 *tal1Δ nqm1Δ trp1Δ*/pXP416-MTOx, pXP420-EEVS)

NQM1 in BY4742 *tal1Δ::KanMX4* was deleted by replacement with a 3.1 Kb PCR amplicon encoding *LEU2*. The *LEU2* amplicon was generated using the NQM1DisLEU2UP/LO primers according to standard methods (Baudin et al. 1993; Gietz and Woods 2001). Transformants were selected on M+his+trp+lys. Deletion of *NQM1* was confirmed by diagnostic PCR using NQM1UP/LO primers to generate a unique 4.2 Kb PCR amplicon. The BY4742 *tal1Δ trp1Δ nqm1Δ* strain was co-transformed with both pXP416-MTOx and pXP420-EEVS using the lithium acetate method (Gietz and Woods 2001). Transformants were selected and maintained on M+leu+lys.

2.3.4 G2C (BY4742 *tal1Δ nqm1Δ trp1Δ*/pXP416, pXP420)

The BY4742 *tal1Δ trp1Δ nqm1Δ* strain was co-transformed with both pXP416 and pXP420 using the lithium acetate method (Gietz and Woods 2001). Transformants were selected and maintained on M+leu+lys.

2.3.5 G3 (*tal1Δ nqm1Δ trp1Δ his3Δ::*pGH420-EEVS-MTOx-2μΔ)

BY4742 *tal1Δ::KanMX4 trp1Δ nqm1Δ* was transformed with *Nde*I-linearized pGH420-EEVS-MTOx-2μΔ to direct integration to the *his3Δ* locus according to standard methods (Gietz and Woods 2001). Transformants were selected on M+lys+trp.

Integration of pGH420-EEVS-MTOx-2μΔ at the *his3Δ* locus was confirmed by diagnostic PCR targeting the junction between *HIS3* and the MTOx gene to generate a 2.3 Kb amplicon using HIS3MTOx-F/R primers.

2.3.6 G4 (BY4742 *tal1Δ nqm1Δ trp1Δ pgi1Δ his3Δ::*pGH420-EEVS-MTOx)

PGI1 in BY4742 *tal1Δ::KanMX4 trp1Δ nqm1Δ his3Δ::*pGH420-EEVS-MTOx-2μΔ was deleted by replacement with a 1.9 Kb PCR amplicon encoding *TRP1*. The *TRP1* amplicon was generated using the PGI1DisTRP1UP/LO primers according to standard protocols (Baudin et al. 1993; Gietz and Woods 2001). Transformants were selected and maintained on YNB + 2% fructose + 0.1% glucose + lys. Deletion of *PGI1* was confirmed by diagnostic PCR using PGI1DisUP/LO primers to generate a unique 3.2 Kb PCR amplicon.

2.3.7 G5 (BY4742 *tal1Δ trp1Δ pgi1Δ his3Δ::*pGH420-EEVS-MTOx)

PGI1 in BY4742 *tal1Δ::KanMX4 trp1Δ* was deleted by replacement with a 1.9 Kb PCR amplicon encoding *TRP1*. The *TRP1* amplicon was generated using the PGI1DisTRP1UP/LO primers according to standard protocols (Baudin et al. 1993; Gietz and Woods 2001). Transformants were selected and maintained on YNB+ 2% fructose + 0.1% glucose + his + leu + lys. Deletion of *PGI1* was confirmed by diagnostic PCR using PGI1DisUP/LO primers to generate a unique 3.2 Kb PCR amplicon. BY4742 *tal1Δ::KanMX4 trp1Δ pgi1Δ* was transformed with *Nde*I-linearized pGH420-EEVS-

MTOx-2μΔ to direct integration to the *his3Δ* locus according to standard methods (Baudin et al. 1993). Transformants were selected on YNB + 2% fructose + 0.1% glucose + leu + lys. Integration of pGH420-EEVS-MTOx-2μΔ at the *his3Δ* locus was confirmed by diagnostic PCR targeting the junction between the *HIS3* marker and the MTOx gene to generate a 2.3 Kb amplicon.

2.3.8 G6 (BY4742 *tal1Δ trp1Δ nqm1Δ shb17Δ/*pXP416-MTOx, pXP420-EEVS)

SHB17 in BY4742 *tal1Δ trp1Δ nqm1Δ* was deleted by replacement with a 1.6 Kb PCR amplicon encoding *HphMX*. *HphMX* was generated using SHB17disHphUP/LO primers according to standard protocols (Baudin et al. 1993; Gietz and Woods 2001). Transformants were selected and maintained on YEPD + hygromycin B. Deletion of *SHB17* was confirmed by diagnostic PCR using SHB17DisUP/LO to generate a unique 2 Kb PCR amplicon. BY4742 *tal1Δ trp1Δ nqm1Δ shb17Δ* was co-transformed with both pXP416-MTOx and pXP420-EEVS according to the lithium-acetate method. Transformants were selected and maintained on M+lys.

2.3.9 G7 (BY4742 *tal1Δ trp1Δ nqm1Δ his3Δ::*pGH420-EEVS-MTOx-2μΔ /pXP416-*SHB17*)

BY4742 *tal1Δ trp1Δ nqm1Δ his3Δ::*pGH420-EEVS-MTOx-2μΔ was transformed with pXP416-*SHB17* according to the lithium-acetate method (Gietz and Woods 2001). Transformants were selected and maintained on M+lys.

2.3.10 G8 (BY4742 *tal1Δ trp1Δ nqm1Δ his3Δ::*pGH420-EEVS-MTOx *TEF1*::pXP416-*SHB17*-2μΔ)

BY4742 *tal1Δ trp1Δ nqm1Δ his3Δ::*pGH420-EEVS-MTOx was transformed with *Bbs*I-linearized pXP416-SHB17-2μΔ to direct integration to the *TEF1* locus according to the lithium-acetate method (Gietz and Woods 2001). The 2μ yeast replicative origin was removed (-2μΔ) to ensure construct integration. Transformants were selected and maintained on M+lys media. Integration of pXP416-SHB17-2μΔ at the *TEF1* locus could not be verified by PCR. However, growth on the selection medium indicates integration of at least the *TRP1* gene with the genome.

2.3.11 G9 (BY4742 *tal1Δ trp1Δ pho13Δ*/pXP416-MTOx, pXP420-EEVS)

PHO13 in BY4742 *tal1Δ trp1Δ* was deleted by replacement with a 1.6 Kb PCR amplicon encoding *HphMX*. The *HphMX* amplicon was generated using the PHO13HphUP/LO primers according to standard methods (Baudin et al. 1993; Gietz and Woods 2001). Transformants were selected on YEPD + hygromycin B. Deletion of *PHO13* was confirmed by diagnostic PCR using PHO13UP/LO primers to generate a unique 2.4 Kb PCR amplicon. The BY4742 *tal1Δ trp1Δ pho13Δ* strain was co-transformed with both pXP416-MTOx and pXP420-EEVS using the lithium acetate method (Gietz and Woods 2001). Transformants were selected and maintained on M+leu+lys.

2.3.12 G10 (BY4742 *tal1Δ trp1Δ*/pXP416-MTOx, pXP420-EEVS, pXP422-ZWF1)

BY4742 *tal1Δ trp1Δ* was transformed with pXP420-EEVS, pXP416-MTOx, and pXP422-ZWF1 according to the lithium-acetate method (Gietz and Woods 2001). Transformants were selected and maintained on M+lys.

2.4 DNA primers

DNA primers needed to construct yeast strains and plasmids are listed in Table 3.

Table 3. DNA primers used for strain and plasmid construction.

Table 3. DNA primers used for strain and plasmid construction.

Name	Sequence (5'->3')	Notes
TRP1DisURA3UP	TATAGGAAGCATTTAATAGAACAGCATCGTAATATATGTGTACTTTGC AGTTATGACGCCGAAATTGAGGCTACTGCGCC	*TRP1*-annealing sequence underlined
TRP1DisURA3LO	CCTGTGAACATTCTCTTCAACAAGTTTGATTCCATTGCGGTGAAATGG TAAAAGTCAACCGGCAGCGTTTTGTTCTTGGA	*TRP1*-annealing sequence underlined
TRP1DisUP	CTCACCCGCACGGCAGAGAC	-
TRP1DisLO	TGCCGGCGGTTGTTTGCAAG	-
NQM1DisLEU2UP	TTCTTGCTAGCGTAAGTCATAAAAAATAGGAAATAATCACATATATAC AAGAAATTAAATCACTGTTCACGTCGCACCTA	*LEU2*-annealing sequence underlined
NQM1DisLEU2LO	ATTATACGTCAGAATTTTAATGAATATATAAGTCTGTACACTATGCTAT GCACATATACTGCTGCATTAATGAAT CGGCCA	*LEU2*-annealing sequence underlined
NQM1DisUP	AAAACTCACATCGCACGCAC	-
NQM1DisLO	GAGCTGAAAGCAATTCTAAATCCA	-
PGI1DisTRP1UP	ACCCAGAAACTACTTTGTTTTTGATTGCTTCCAAGACTTTCACTACCG CTGAAACTATCAATGCGTAAGGAGAAAATACC	*TRP1*-annealing sequence underlined
PGI1DisTRP1LO	AGATAGAACCAGTAGAGTAGTCAGTAAACACGTTACCTCTGGTAACA GACTTACCGTTAGATGCAGCTCAGATTCTTTGT	*TRP1*-annealing sequence underlined
PGI1DisUP	GGCAAGAACCGGGATGGTAA	-
PGI1DisLO	TGTAGTTACTTGGACGCTGTTC	-
SHB17DisHphUP	AGCACATTTTGTTCATAGCTAAGTGGATAGGGAAACACCTACACTTAA TTGCAAGCAACAGGGCATGATGTGACTGTCGCCC	*HphMX*-annealing sequence underlined
SHB17DisHphLO	AAAAAATGTTTTTATCACTTTCTATAACTGCATATCTTTTTTTGCATTTC GAATGATTGCTCTGGGCAGATGATGTCGAGGC	*HphMX*-annealing sequence underlined
SHB17DisUP	CCACCGCCAAATTGCTATCC	-
SHB17DisUP	ACAGTCCTTTGTACTATCCCTTTTA	-
PHO13HphUP	AGCCAAATCACAAAAAAAGCCTTATAGCTTGCCCTGACAAAGAATATA CAACTCGGGAAAGGGCATGATGTGACTGTCGCCC	*HphMX*-annealing sequence underlined
PHO13HpHLO	AAACCTGAATATTTTTCCTTTTCAAAAAGTAATTCTACCCCTAGATTTT GCATTGCTCCTTCTGGGCAGATGATGTCGAGGC	*HphMX*-annealing sequence underlined
PHO13Up	AAGTGGCTTGAGCTGTGGAT	-
PHO13LO	GGTTCTTCTGCTGCATTAGGC	-
MTOXUP	AGATCCACTAGTATGCAAACGGCAAAAGTCTC	*Spe*I site underlined
MTOXLO	TAGCCACTCGAGTCACCACAGAGACTGACCG	*Xho*I site underlined

Table 3. DNA primers used for strain and plasmid construction. (Continued)

Name	Sequence (5'->3')	Notes
PTEF1-Spe1-SHB17	TTCTTGCTCATTAGAAAGAAAGCATAGCAATCTAATCTAAGTTTTAATTACAAAACTAGT ATGCCTTCGCTAACCCCC	*pXP416*-annealing sequence underlined
TCYC1-XhoI-SHB17	GAGCGGATGTGGGGGGAGGGCGTGAATGTAAGCGTGACATAACTAATTACATGACTCGAG TTACACATCGCCATGCTGGG	*pXP416*-annealing sequence underlined
DEEVSUP	AGATCCACTAGTATGGAACGTCCGGGCGAAAC	*Spe*I site underlined
DEEVSLO	TAGCCACTCGAGTCACTGCGGTGAGCCGGT	*Xho*I site underlined
A-HIS3-F	ACTATATGTGAAGGCATGGCTATGGCACGGCAGACATTCCGCCAGATCATCAATAGGCACcttcattcaacgtttcccatt	Paired with B-HIS3-R
B-HIS3-R	GTTGAACATTCTTAGGCTGGTCGAATCATTTAGACACGGGCATCGTCCTCTCGAAAGGTGtgatgcattaccttgtcatc	Paired with A-HIS3-F
B-PPGK1-FII	ACCTTTCGAGAGGACGATGCCCGTGTCTAAATGATTCGACCAGCCTAAGAATGTTCAACcctgacttcaactcaagacgc	Paired with MT-P_{PGK1}-RII
MT-P_{PGK1}-RII	CAGCAGATGTTCCACAATAAATTCAACCGGGGTGTCCGAGACTTTTGCCGTTTGCATactagtatatttgttgtaaaaagtagataattacttcc	Paired with B-PPGK1-FII
MTOx-F	ACGTCTCACGGATCGTATATGCCGTAGCGACAATCTAAGAACTATGCGAGGACACGCTAGactagtatgcaaacggcaaaagtctc	Paired with MTOx-R
MTOx-R	AATCACTCTCCATACAGGGTTTCATACATTTCTCCACGGGACCCACAGTCGTAGATGCGT ctcgagtcaccacagagactgaccg	Paired with MTOx-F
Ox-T_{PGK1}-FII	GCATCCGACTACATGACCGGTCACAATCTGGTTATTGAAGGCGGTCAGTCTCTGTGGTGA attgaattgaattgaaatcgatagatca	Paired with C-T_{PGK1}-RII
C-T_{PGK1}-RII	GCCTACGGTTCCCGAAGTATGCTGCTGATGTCTGGCTATACCTATCCGTCTACGTGAATAttttgttgcaagtgggatga	Paired with Ox-T_{PGK1}-FII
C-2μ-F	TATTCACGTAGACGGATAGGTATAGCCAGACATCAGCAGCATACTTCGGGAACCGTAGGC gaattcgtatgatccaatatc	Paired with D-2μ-R
D-2μ-R	TGCCGAACTTTCCCTGTATGAAGCGATCTGACCAATCCTTTGCCGTAGTTTCAACGTATG gaattcaacgaagcatctgtgc	Paired with C-2μ-F
D-ORI-F	CATACGTTGAAACTACGGCAAAGGATTGGTCAGATCGCTTCATACAGGGAAAGTTCGGCAaaaggcggtaatacggtta	Paired with E-AMP-R
E-AMP-R	GTCACGGGTTCTCAGCAATTCGAGCTATTACCGATGATGGCTGAGGCGTTAGAGTAATCTgaaaaaggaagagtatgagtattc	Paired with D-ORI-F
E-PTEF1-F	AGATTACTCTAACGCCTCAGCCATCATCGGTAATAGCTCGAATTGCTGAGAACCCGTGAC accgcgaatccttacatcac	Paired with A-TCYC1-RII
A-TCYC1-RII	GTGCCTATTGATGATCTGGCGGAATGTCTGCCGTGCCATAGCCATGCCTTCACATATAGTcagacaagctgtgaccgtct	Paired with E-PTEF1-F
HIS3MTOx-F	CTTGGATTTATGGCTCTTTTGG	Confirmation of pGH420-EEVS-MTOx-2μΔ integration
HIS3MTOx-R	CTTAGCCTTCAGCAGATGTTCC	Confirmation of pGH420-EEVS-MTOx-2μΔ integration
ZWF1SpeIUP	AGATCCACTAGTATGAGTGAAGGCCCCGTC	*Spe*I restriction site underlined
ZWF1XhoILO	AGATCCCTCGAGCTAATTATCCTTCGTATCTTC	*Xho*I restriction site underlined

2.5 Construction of plasmids

Plasmids (Table 4) were constructed as described below. Plasmid maps are shown in Fig. 8-12.

Table 4. Plasmids.

Plasmid	Feature	*E. coli* carrier	Source/reference
pRSETB-EEVS	EEVS (*Eco*RV)	BL-21	(Osborn et al. 2015)
pRSETB-MTOX	MTOx (*Eco*RV	BL-21	(Osborn et al. 2015)
pXP416	*TRP1*; *TEF1* promoter	DH5α	(Fang et al. 2011)
pXP416-MTOx	MT-Ox (*Spe*I+*Xho*I)	NEB-10β	(Osborn et al. 2015)
pXP416-SHB17	*SHB17*	TOP10	This study
pXP416-SHB17-2μΔ	*SHB17,* and missing 2μ ORI	TOP10	This study
pXP420	*HIS3; TEF1* promoter	DH5α	(Fang et al. 2011)
pXP420-EEVS	EEVS (*Spe*I+*Xho*I)	TOP10	(Osborn et al. 2015)
pGH420-EEVS-MTOx	EEVS, MT-Ox	TOP10	This study
pGH420-EEVS-MTOx-2μΔ	EEVS, MT-Ox, and missing 2μ ORI	TOP10	This study
pXP422	*LEU2; TEF1* promoter	TOP10	(Fang et al. 2011)
pXP422-ZWF1	*ZWF1*	NEB-5α	This study

2.5.1 pXP416-MTOx

pXP416 plasmid was extracted and purified from a 1-ml culture of DH5α/pXP416 *E. coli* grown in LB+amp. An aliquot of pXP416 was digested with *Spe*I- and *Xho*I-restriction enzymes yielding a 5.8 Kb fragment. *Spe*I-, *Xho*I-digested plasmid was gel purified using a Qiagen gel-purification kit. The MTOx cDNA was amplified by PCR from

pRSETB-MTOx yielding a 1.7 Kb amplicon. The MTOXUP/MTOXLO primers used for amplification attached a *Spe*I site to the 5'-end and a *Xho*I site to the 3'-end of the cDNA. The MTOx PCR amplicon flanked by *Spe*I and *Xho*I sites was digested with *Spe*I and *Xho*I and gel purified using a gel-purification kit (Qiagen). The purified *Spe*I-*Xho*I-digested MTOx cDNA was ligated into *Spe*I-*Xho*I-digested pXP416 using New England Biolab's T4 DNA ligase kit. The ligation mixture was used to transform competent TOP10 *E. coli* (Invitrogen). Transformants were selected and maintained on LB+amp plates. Construction of pXP420-MTOx (Fig. 8) was confirmed by digesting purified plasmid DNA with *Spe*I and *Xho*I to yield 5.8 and 1.7 Kb fragments.

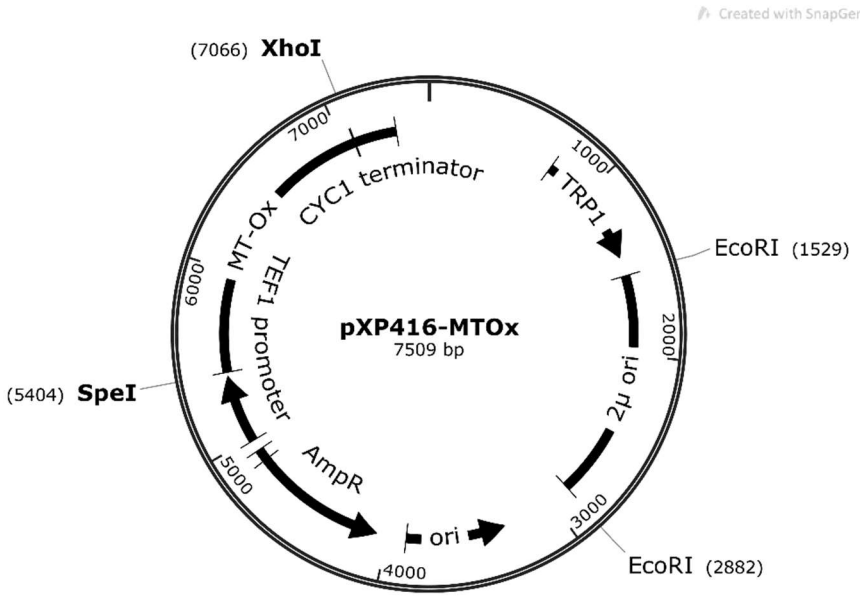

Figure 8. pXP416-MTOx.

2.5.2 pXP416-*SHB17*

SHB17 was cloned into pXP416 by homologous recombination to avoid disrupting the *SHB17* ORF by cutting with *Xho*I. *SHB17* was amplified using PTEF1-Spe1-SHB17/TCYC1-XhoI-SHB17 primers that contained 60-bp of sequence homologous to both ends of *Spe*I-*Xho*I-linearized pXP416. BY4742 *tal1Δ trp1Δ* was

transformed with *SHB17* amplicon and *Spe*I-*Xho*I linearized pXP416 plasmid according to standard methods (Gietz and Woods 2001). Transformants were selected and maintained on M+his+leu+lys. The plasmid was rescued from a yeast transformant by extracting DNA according to a genomic DNA extraction protocol and used to transform competent TOP10 *E. coli* (Schwartz and Sherlock 2016). Plasmid DNA was extracted and purified from *E. coli* transformants using a plasmid miniprep kit (Qiagen). Construction of pXP416-*SHB17* was verified by digestion with *Bbs*I and analysis by gel electrophoresis which yielded 2.8 and 3.8 Kb fragments as expected. The DNA sequence for *SHB17* can be found in appendix 6.4.3.

2.5.3 pXP416-*SHB17*-2μΔ

The yeast origin of replication (2μΔ) sequence was removed from pXP416-*SHB17* by digestion with *Eco*RI. Five nanograms of *Eco*RI-digested pXP416-*SHB17* DNA were added to a T4 ligase-mediated ligation reaction after which competent TOP10 *E. coli* was transformed with 5 μl of the reaction mixture. Transformants were selected on LB+Amp. Construction of pXP416-

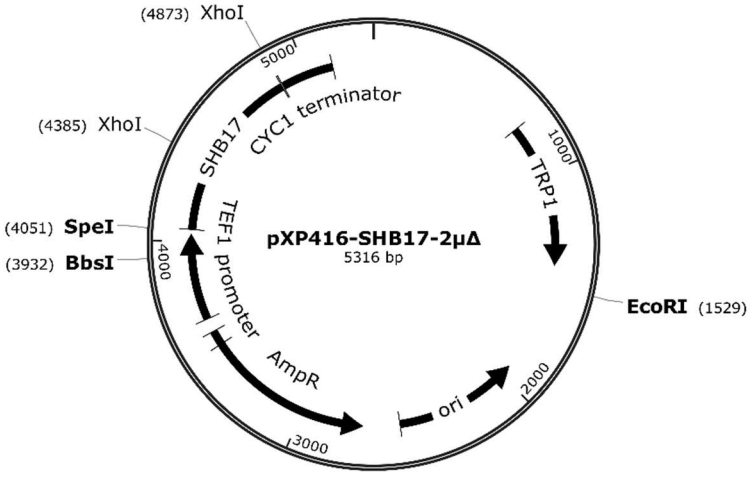

Figure 9. pXP416-SHB17-2μΔ.

SHB17-2μΔ (Fig. 9) was confirmed by digestion with *Bbs*I and analyzed by gel electrophoresis which indicated a 5.3 Kb fragment.

2.5.4 pXP420-EEVS

pXP420 plasmid was extracted and purified from a 1-ml culture of DH5α/pXP420 *E. coli* grown in LB+amp. An aliquot of pXP420 was digested with *Spe*I- and *Xho*I-restriction enzymes yielding a 6.0 Kb fragment.

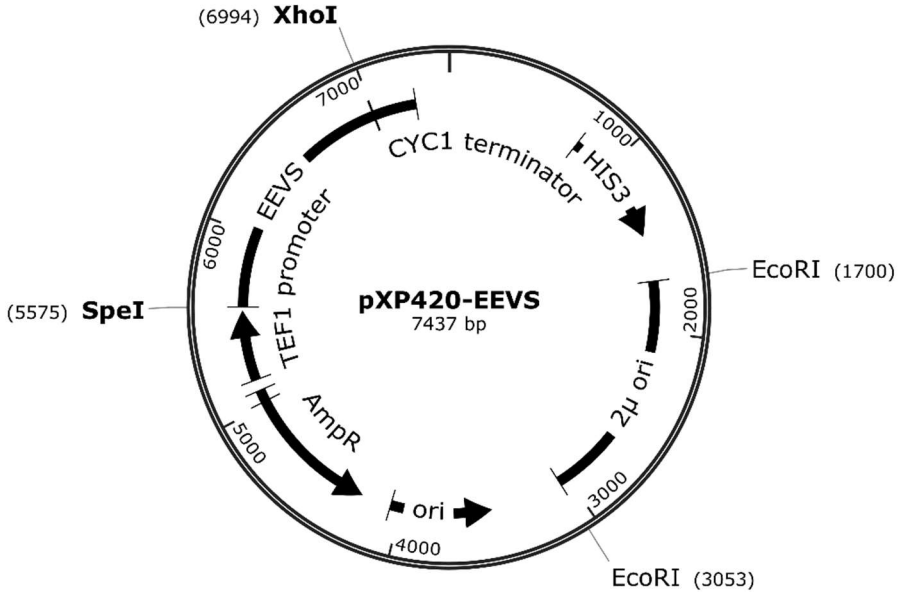

Figure 10. pXP420-EEVS

*Spe*I-, *Xho*I-digested plasmid was gel purified using a Qiagen gel-purification kit. The EEVS cDNA was amplified by PCR from pRSETB-EEVS yielding a 1.4 Kb amplicon. The DEEVSUP/DEEVSLO primers used for amplification attached a *Spe*I site to the 5'-end and a *Xho*I site to the 3'-end of the cDNA. The EEVS PCR amplicon bordered by *Spe*I and *Xho*I sites was digested with *Spe*I and *Xho*I and gel purified using a Qiagen gel-purification kit. The purified *Spe*I-*Xho*I digested EEVS cDNA was ligated into *Spe*I-*Xho*I digested pXP420 using New England Biolab's T4 DNA ligase kit. The ligation mixture was then used to transform competent TOP10 *E. coli* from Invitrogen.

Transformants were selected and maintained on LB+amp plates. Construction of pXP420-EEVS (Fig. 10) was confirmed by digesting purified plasmid DNA with *Spe*I and *Xho*I to yield 6.0 and 1.4 Kb fragments.

2.5.5 pGH420-EEVS-MTOx

A plasmid expressing both EEVS and MTOx was constructed using *in vivo* ligation. BY4742 *tal1Δ trp1Δ nqm1Δ* was co-transformed with seven PCR amplicons as described in appendix 6.1. Yeast transformants were selected on M+trp+lys. Plasmid DNA was purified from a yeast transformant and used to transform *E. coli.* Transformants were selected on LB+amp and verified as described in the appendix 6.1.

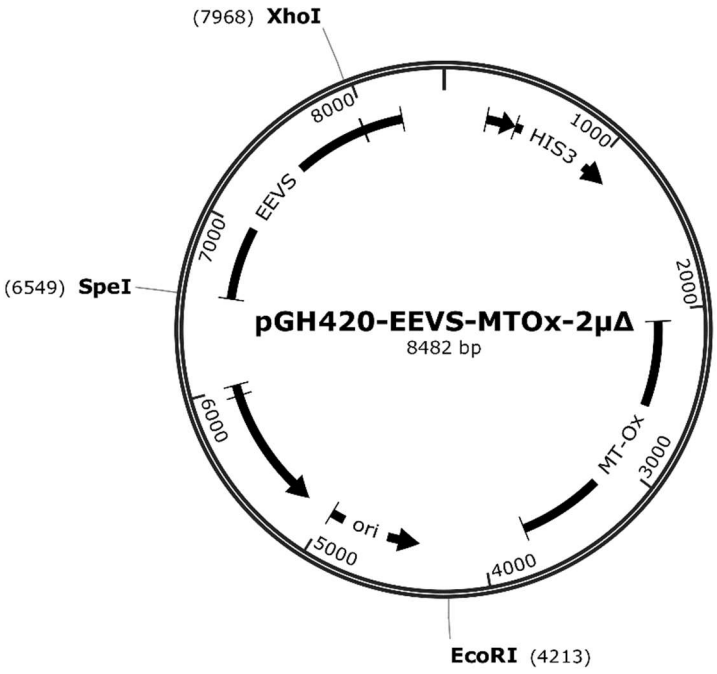

Figure 11. pGH420-EEVS-MTOx-2μΔ.

2.5.6 pGH420-EEVS-MTOx-2μΔ

To facilitate stable integration of the pGH420-EEVS-MTOx plasmid into the yeast genome the yeast origin of replication (2μ) was first digested with *Eco*RI restriction enzyme for

Sequences for the EEVS and MTOx cDNAs can be found in appendix 6.4.

30 min at 37 ºC. *Eco*RI-digested pGH420-EEVS-MTOx was then heated to 65ºC for 20 min to inactivate enzyme. Digested plasmid was diluted 20-fold in a T4 DNA ligase reaction to circularize the construct without the 2μ sequence (Fig. 11). Competent TOP10 *E. coli* was transformed with 5 μl of the ligation mixture. Transformants were selected and maintained on LB+amp plates. Construction of pGH420-EEVS-MTOx-2μΔ was confirmed by digestion with *Eco*RI which yielded an 8.5 Kb fragment by gel electrophoresis.

2.5.7 pXP422-*ZWF1*

pXP422 plasmid was extracted and purified from a 1-ml culture of TOP10/pXP420 *E. coli* grown in LB+amp. An aliquot of pXP422 was digested with *Spe*I- and *Xho*I-restriction enzymes yielding a 6.3 Kb fragment. *Spe*I-, *Xho*I-digested plasmid was gel purified using a Qiagen gel-purification kit. The *ZWF1* gene was amplified by PCR from BY4742 yielding a 1.5 Kb amplicon. The ZWF1SpeIUP/ZWF1XhoILO primers used for amplification attached a *Spe*I site to the 5'-end and a *Xho*I site to the 3'-end of the gene. The *ZWF1* PCR amplicon bordered by *Spe*I and *Xho*I sites was digested with

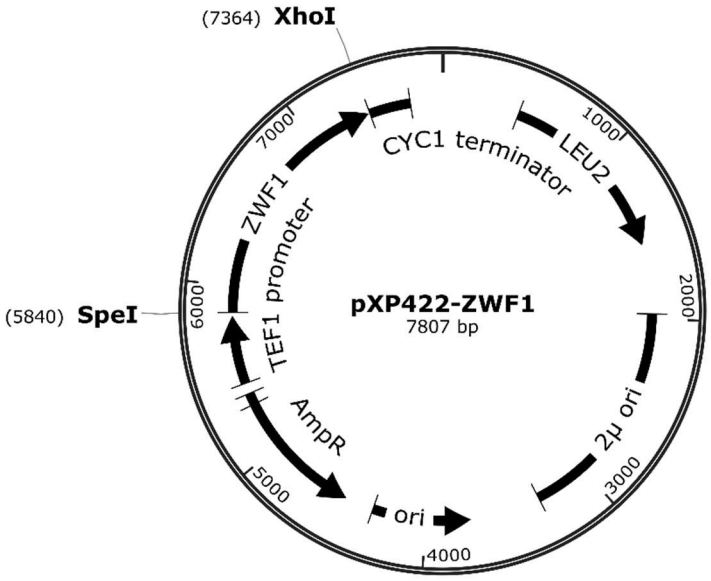

Figure 12. pXP422-ZWF1

*Spe*I and *Xho*I and gel purified using a Qiagen gel-purification kit. The purified *Spe*I-*Xho*I digested *ZWF1* gene was ligated into *Spe*I-*Xho*I digested pXP422 using New England Biolab's T4 DNA ligase kit. The ligation mixture was then used to transform competent TOP10 *E. coli* from Invitrogen. Transformants were selected and maintained on LB+amp plates. Construction of pXP422-ZWF1 (Fig. 12) was confirmed by digesting purified plasmid DNA with *Spe*I and *Xho*I to yield 6.3 and 1.5 Kb fragments. The DNA sequence for *ZWF1* can be found in appendix 6.4.4.

2.6 Measurements of biomass and gadusol

Yeast biomass was monitored spectrophotometrically at A_{600} using a UV-visible spectrophotometer (Shimadzu UV-1601). Cultures were diluted with distilled water such that the measured values did not exceed 0.3 because previous measurements had shown this to be the limit of linearity for this spectrophotometer. Actual A_{600} values were calculated by multiplying by the dilution factor. Exit from log phase was determined to estimate when gadusol production was relative to growth. Exit from log phase was estimated by finding the intersection of an exponential growth trend line fitted to cultures in log phase and a polynomial trend line fitted to cultures exiting log phase (Microsoft Excel, Redmond, WA). An example featuring strain G2 may be found in appendix 6.5.

To measure extracellular gadusol from a culture, yeast cells were pelleted and a sample of culture supernatant was diluted to 50 mM phosphate, pH 7. The absorbance of the supernatant was measured at 296 nm using distilled water as a blank. Gadusol concentrations were calculated according to Beer's law using gadusol's extinction

coefficient, 21,800 M^{-1} cm^{-1} at pH 7 in 50 mM phosphate. This value was determined previously for a gadusol sample of undefined purity (Plack et al. 1981). The formula below accounts for background absorbance at 296 nm due to non-gadusol components in the fermentation. The average A_{296}/A_{600} ratio (0.0537) of a control strain (G2C) grown in triplicate for three days at 30ºC and 200 RPM, was subtracted from the A_{296}/A_{600} ratio of a sample to correct for background A_{296} absorbance. The difference in ratios was then multiplied by the sample's A_{600}, giving absorbance from gadusol which was then divided by gadusol's extinction coefficient (21,800 M^{-1} cm^{-1}) to determine molarity.

$$\text{Gadusol (M)} = \frac{\left[\left(\frac{A_{296}}{A_{600}}\right)_{\text{Gad}} - 0.0537\right] \text{X } (A_{600})_{\text{Gad}}}{21{,}800\ \text{M}^{-1}\text{cm}^{-1}}$$

$(A_{296})_{Gad}$= The A_{296} of a yeast culture supernatant as described in the preceding section.

$(A_{600})_{Gad}$= The A_{600} of a yeast culture as described in the preceding section.

2.7 Statistical analysis

Statistical significance (p<0.05) of differences was determined using Student's two-tailed, paired *t* test (Microsoft Excel, Redmond, WA).

3 Results and Discussion

The gadusol biosynthetic pathway in vertebrates was recently shown to originate from the pentose phosphate pathway intermediate S7P and to require two enzymes: EEVS and bifunctional MT-Ox (Osborn et al. 2015). cDNAs encoding the two genes from zebrafish (*Danio rerio*) were expressed in *E. coli* and were shown to mediate the in vitro conversion of S7P to EEV, and the SAM- and NAD^+-dependent conversion of EEV to gadusol, respectively. In order to explore the possibility of producing gadusol in yeast, the cDNAs were sub-cloned into the yeast expression vectors pXP420 and pXP416 to yield pXP420-EEVS and pXP416-MTOx, respectively. Both vectors contained the same strong constitutive *S. cerevisiae* promoter, *TEF1*, but different selectable markers. Table 5 lists a set of gadusol-producing strains that were constructed and provides characteristics related to growth and gadusol yields. Although the strains have been numbered, no relationship is necessarily implied based on the numerical designation. Strains and interventions that increased gadusol yields are presented earlier in the table and reflect their position in the text, while the remaining strains and interventions follow.

Table 5. Growth and gadusol production by constructed yeast strains.

[1]Student's two-tailed, paired *t* test was performed to determine the significance ($p<0.05$) of differences between 1) doubling time, 2) final biomass (A_{600}) values, and 3) final gadusol (mg/L) yields among all strains. **Means within the same column** that are followed by different superscripts are significantly different.

Table 5. Growth and gadusol production by constructed yeast strains.

Strain	Conditions	Doubling time (h)[1]	End of log phase (h)	Gadusol made (%) after exiting log phase	Time to reach maximal gadusol (h)	Biomass (A_{600}) at maximal gadusol[1]	Maximal gadusol (mg/L)[1]	Feature
G0	YNB+2%glu+leu+lys	2.0±0.1^{a}	17	96	110	1.30±0.03^{a}	11.9±0.1^{a}	*TAL1 NQM1*/pXP416-MTOx, pXP420-EEVS
G1	YNB+2%glu+leu+lys	3.6±0.4^{b}	26	87	110	1.42±0.04^{a}	22.4±0.9^{b}	*tal1Δ NQM1/* pXP416-MTOx, pXP420-EEVS
G10	YNB+2%glu+lys	3.0±1.4^{abcd}	39	93	207	3.31±0.47^{bcfg}	36.7±1.5^{i}	*tal1Δ NQM1/*pXP422-*ZWF1,* pXP416-MTOx, pXP420-EEVS
G2	YNB+2%glu+lys	3.5±0.1^{b}	33	93	130	3.07±0.08^{b}	30.1±0.2^{c}	*tal1Δ nqm1Δ* /pXP416-MTOx, pXP420-EEVS
G3	YNB+2%glu+lys+trp	1.7±0.0^{c}	15	96	169	3.54±0.42^{c}	64.1±7.5^{d}	*tal1Δ nqm1Δ his3Δ1*::pGH420-EEVS-MTOx-2μΔ
G3	2Xlys+2Xtrp	2.1±0.7^{acd}	24	86	155	5.53±0.20^{d}	65.7±1.4^{de}	*tal1Δ nqm1Δ his3Δ1*::pGH420-EEVS-MTOx-2μΔ
G3	2Xtrp	2.5±0.1^{d}	27	85	155	5.00±0.13^{eh}	66.5±6.3^{def}	*tal1Δ nqm1Δ his3Δ1*::pGH420-EEVS-MTOx-2μΔ
G3	2Xlys	2.3±0.0^{d}	23	88	131	3.50±0.29^{bcf}	63.3±3.9^{def}	*tal1Δ nqm1Δ his3Δ1*::pGH420-EEVS-MTOx-2μΔ
G9	YNB+2%glu+leu+lys	3.6±0.2^{b}	35	95	186	1.56±0.05	13.7±0.4^{h}	*tal1Δ NQM1 pho13Δ*/pXP416-MTOx, pXP420-EEVS
G6	YNB+2%glu+lys	5.9±0.6^{f}	60	74	156	2.91±0.06^{b}	17.9±0.6^{h}	*tal1Δ nqm1Δ shb17Δ*/pXP416-MTOx, pXP420-EEVS
G7	YNB+2%glu+lys	4.4±0.1^{g}	48	84	106	4.76±0.15^{h}	28.4±3.5^{c}	*tal1Δ nqm1Δ his3Δ1*::pGH420-EEVS-MTOx-2μΔ/pXP416-*SHB17*
G8	YNB+2%glu+lys	2.0±0.0^{ad}	17	98	208	3.44±0.22^{bcf}	60.6±2.5^{dfg}	*tal1Δ nqm1Δ his3Δ1*::pGH420-EEVS-MTOx-2μΔ pXP416-*SHB17* integrant
G3	NADPH nutr.	2.6±0.1^{d}	32	85	230	3.67±0.14^{cf}	67.8±2.2^{def}	*tal1Δ nqm1Δ his3Δ1*::pGH420-EEVS-MTOx-2μΔ
G4	YNB+2%fru+0.1%glu+lys	8.6±0.4^{e}	47	83	264	2.56±0.06^{g}	53.0±4.7^{g}	*tal1Δ nqm1Δ pgi1Δ his3Δ1*::pGH420-EEVS-MTOx-2μΔ
G5	YNB+2%fru+0.1%glu+leu+lys	4.2±0.5^{b}	39	90	302	0.93±0.21^{i}	15.1±3.0^{h}	*tal1Δ NQM1 pgi1Δ his3Δ1*::pGH420-EEVS-MTOx-2μΔ

3.1 EEVS and MTOx expression is sufficient for gadusol synthesis in *S. cerevisiae*

A *trp1*∆ derivative of the laboratory haploid BY4742 was co-transformed with both plasmids to generate strain G0 that was found to produce 12 mg/L of gadusol after 110 h (Fig. 13). Comparing G0 to a standard haploid laboratory strain, S288c *leu2Δ/*pGP564 grown in YNB +2% glucose, pH 4.8 (t_d=2.0 vs 2.0 h), shows that expression of EEVS and MTOx is not particularly costly for yeast (Ding et al. 2015). To determine whether deletion of the major yeast transaldolase gene *TAL1* would increase yields by eliminating an important S7P-consuming reaction, strain G1 was constructed that lacked Tal1 activity but still expressed *EEVS* and *MTOx*. G1 (*tal1*∆) was found to produce 22 mg/L after the same 110 h (Fig 13). While G1 produced almost twice as much gadusol as G0, it grew more slowly than G1 (t_d=3.6 vs 2 h), but reached about the same final cell titer (A_{600} = 1.4 vs 1.3). The increase in doubling time between G0 and G1 could be explained by the loss of Tal1 activity, which would lead to decreased throughput in the PPP and availability of intermediates needed for producing biomass (E4P, and R5P).

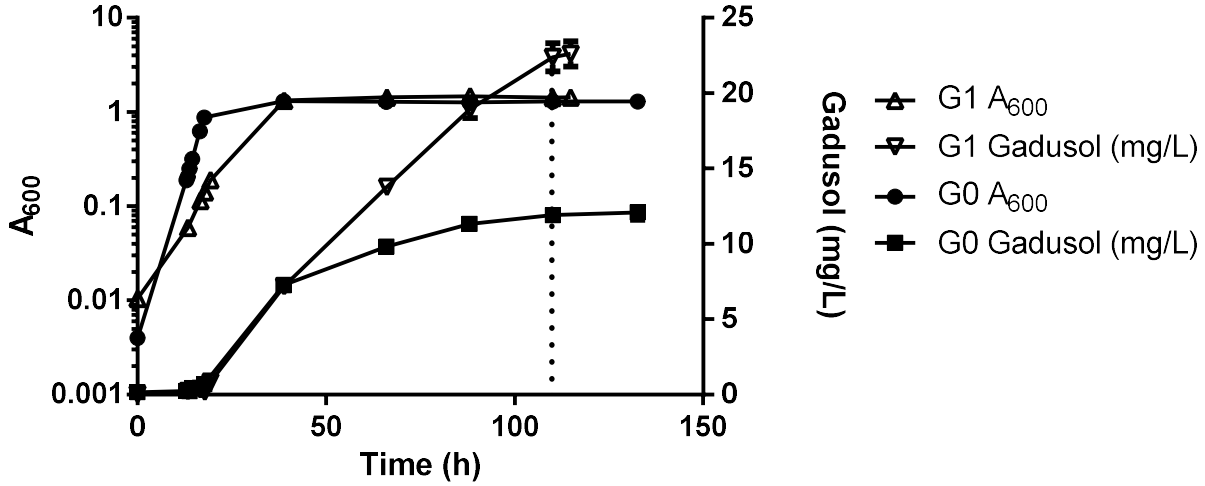

Figure 13. Growth and gadusol production by G0 (*TAL1*) and G1 (*tal1Δ*). Maximal measurements for gadusol and biomass were taken at 110 h as indicated by the dashed line. Error bars are standard deviations.

3.2 Overexpression of ZWF1 increases gadusol production

ZWF1 encodes glucose 6-P dehydrogenase which catalyzes the first step in the oxidative phase of the PPP (Stincone et al. 2015). A *ZWF1*-overexpressing mutant (G10) was constructed in the G1 background (*tal1Δ*) because it is thought to be the rate-limiting step in the PPP (Ralser et al. 2007; Stincone et al. 2015). I reasoned that overexpressing *ZWF1* would divert more glucose 6-P from glycolysis to the PPP to form more S7P, the gadusol precursor. Figure 14 compares growth and gadusol yield for the G1 (*tal1*Δ) and G10 (*tal1*Δ/pXP422-*ZWF1*) strains to allow assessment of the contribution of *ZWF1* overexpression.

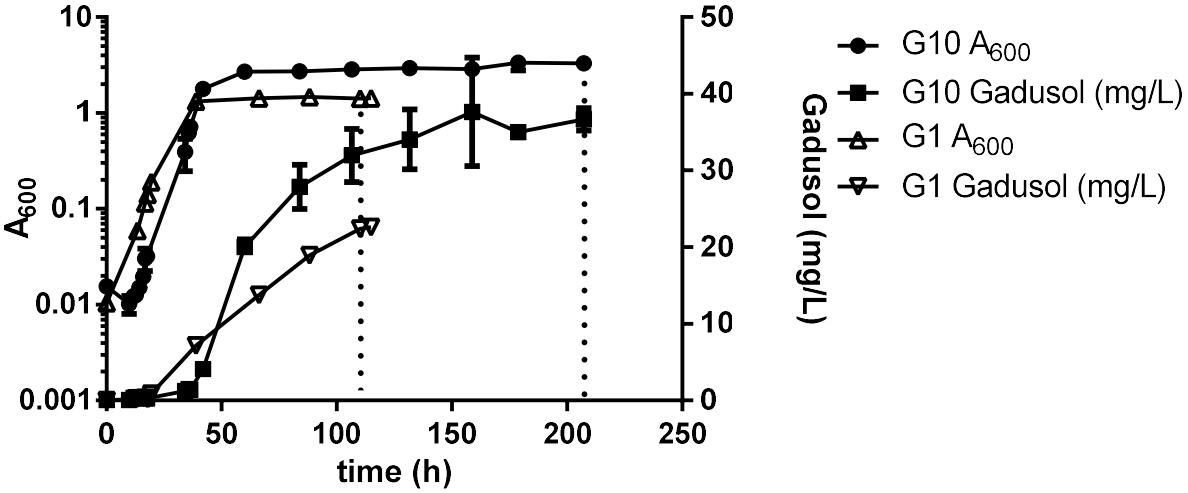

Figure 14. Growth and gadusol production by G1 (*tal1Δ*) and G10 (*tal1Δ*/pXP422-*ZWF1*). Maximal gadusol and biomass measurements for G10 and G1 were taken at 207 and 110 h, respectively (dashed lines). Error bars are standard deviations.

The G10 strain produced 37 mg/L of gadusol compared to 22 mg/L for G1, a 68% increase (Fig. 14). However, G10 required 207 h to reach this higher concentration. It is not clear if gadusol production by G1 would have continued to increase after the final measurement was taken for this strain at 110 h. G10 grew faster than G1 (t_d = 2.6 vs 3.6 h) and produced 2.4 times more cells (A_{600} = 3.3 vs 1.4). This latter observation indicates greater carbon assimilation by the *ZWF1*-overexpressing G10 strain, consistent with a more active PPP.

3.3 Elimination of a second transaldolase gene NQM1 increases gadusol yield

NQM1 encodes a paralogue of *TAL1* (Huang et al. 2008). While the encoded enzyme is not active during fermentative growth on glucose, it is heavily transcribed during respiratory growth on glycerol (21, 31). I reasoned that deletion of *NQM1* would eliminate all known transaldolase activity and increase gadusol yields. To this end, the G2 strain (*tal1*Δ *nqm1*Δ) was constructed and compared to G1 (*tal1*Δ).

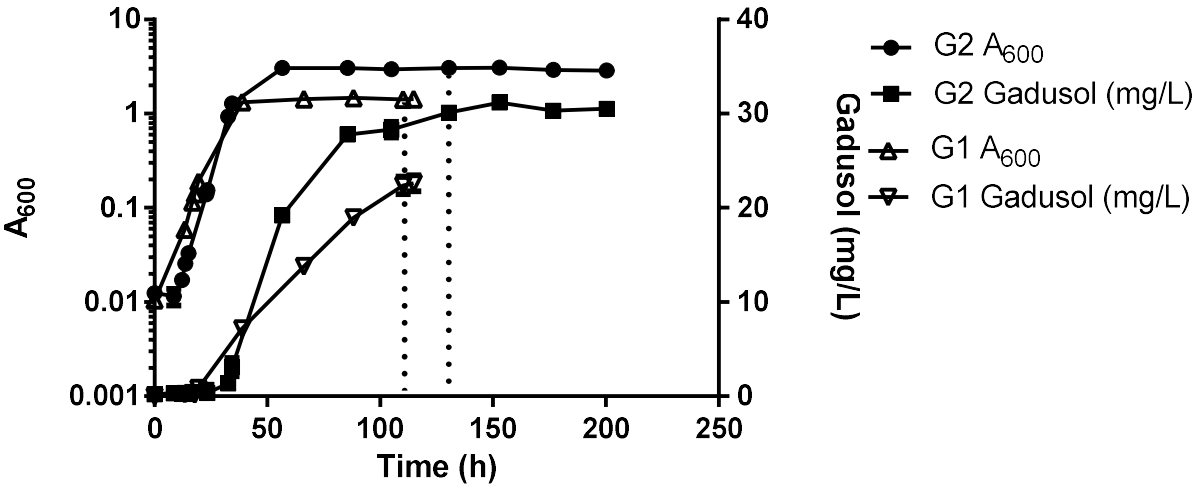

Figure 15. Growth and gadusol production by G1 (*tal1Δ NQM1*) and G2 (*tal1Δ nqm1Δ*). Maximal gadusol and biomass measurements for G1 and G2 were taken at 110 and 130 h, respectively (dashed lines). Error bars are standard deviations.

The G2 strain produced 30 vs 22 mg/L of gadusol or 36% more than G1, but required 130 h to reach this level. While the two strains grew at about the same rate (t_d ~ 3.5 h), G2 produced twice as much biomass as G1 (A_{600} = 3.1 vs 1.4). It is likely that decreased throughput in the PPP blocked by a lack of transaldolase activity elevated levels of ribose 5-P which in turn fueled greater carbon assimilation. G2 produced more than twice the gadusol made by G1 during stationary phase.

3.4 Chromosomal integration of a plasmid carrying EEVS and MTOx leads to increased gadusol production

The limited number of genetic markers available in the G2 strain necessitated redesigning the gadusol expression system. In order to eliminate the need for two plasmids (and two genetic markers), both *EEVS* and *MTOx* genes were cloned into a single plasmid by *in vivo* ligation to generate pGH420-EEVS-MTOx. The plasmid was then converted into an integrative construct by excision of the 2μ yeast origin of replication. The pGH420-EEVS-MTOx-2μΔ construct was digested with *Nde*I and used to transform a *tal1*Δ *nqm1*Δ yeast mutant. Prior digestion with *Nde*I was meant to facilitate integration of the construct at the *Nde*I site in the *his3Δ1* locus. The resultant strain was designated G3 (Fig. 16).

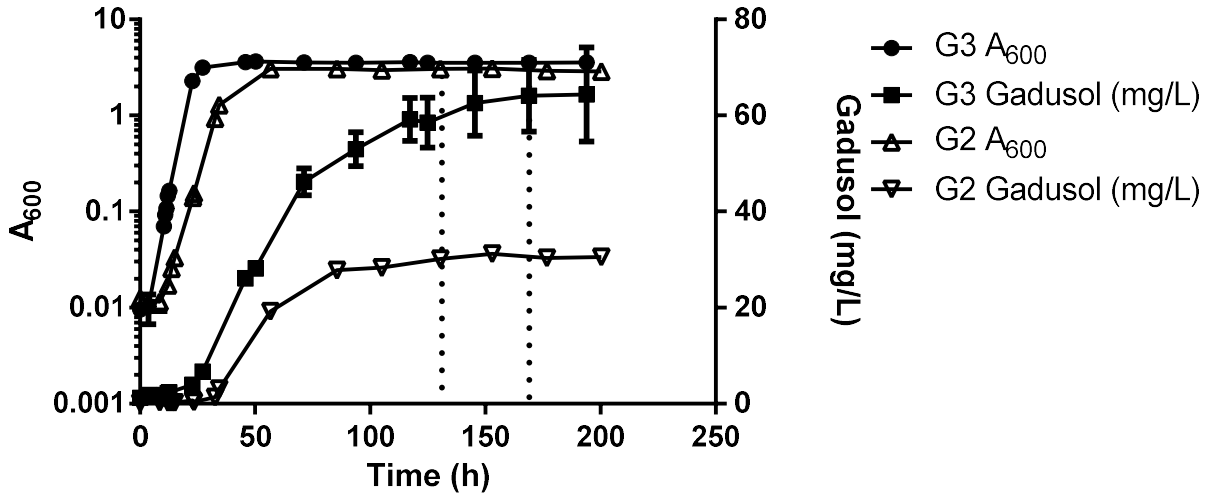

Figure 16. Growth and gadusol production by G2 (*tal1Δ nqm1Δ*) and G3 (*tal1Δ nqm1Δ his3Δ1*::pGH420-EEVS-MTOx). Maximal gadusol and biomass measurements for G2 and G3 were taken at 130 and 169 h, respectively (dashed lines). Error bars are standard deviations.

The G3 strain produced 64 vs 30 mg/L of gadusol or 113% more than G2, but required 169 h to reach this concentration. In contrast, G2 reached 30 mg/L by 130 h. G3 grew much faster than G2 (t_d = 1.6 vs 3.5 h), but did not produce significantly more biomass, (A_{600} = 3.5 vs 3.1). The observation that G3 grew more than two times faster than G2 and that the only difference between the strains was the integrated construct vs two high copy plasmids suggests that the plasmids caused growth inhibition. Inclusion of constitutive glycolytic promoters on plasmids has been reported to reduce yeast growth rates by 12-15% (Görgens et al. 2001). In this particular case, the authors speculated that multiple copies of plasmid-borne constitutive promoters could attenuate

the transcriptional machinery by titrating a limited number of transcription factors and RNA polymerases which would normally exist in excess.

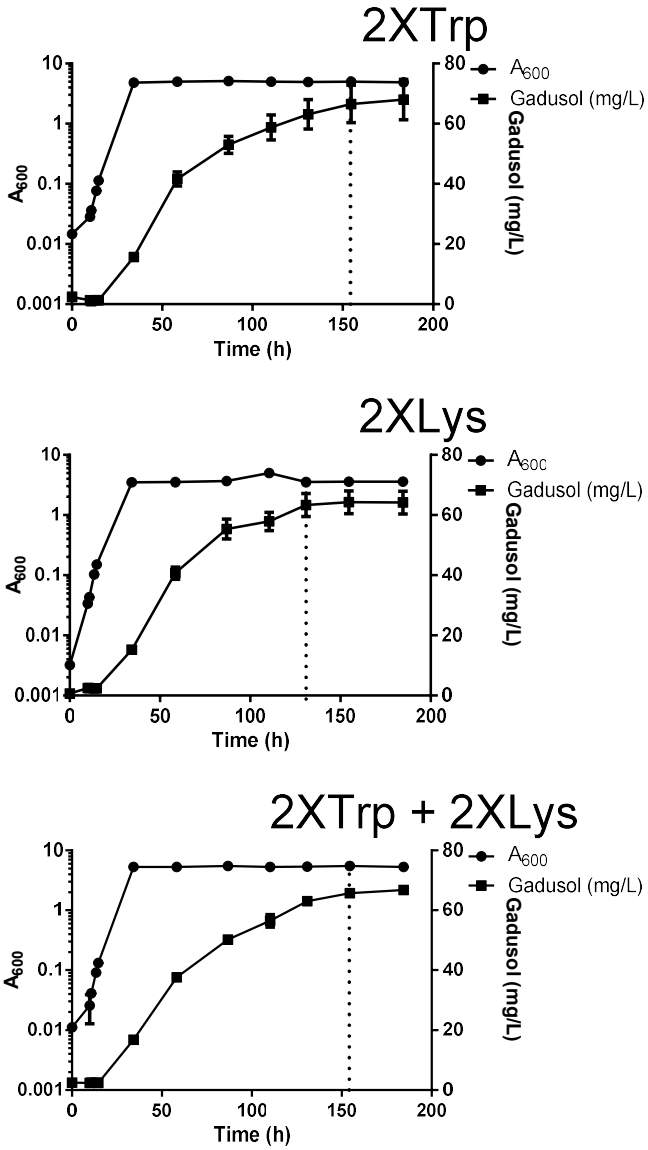

3.5 Supplementation with the growth-limiting nutrients tryptophan and lysine has no effect on gadusol yield

Supplementing growth medium with the nutrients lysine (Lys) and tryptophan (Trp) was tested as a means to increase gadusol production. Supplementation had no significant effect on gadusol production by G3 (64 vs 63-67 mg/L).

Figure 17. Growth and gadusol production by G3 (tal1Δ nqm1Δ his3Δ1::pGH420-EEVS-MTOx) in YNB + 2% glucose supplemented with 2XTrp + 2XLys, 2XTrp, and 2XLys. Maximal gadusol and biomass measurements for the 2XTrp + 2XLys and 2XTrp treatments were taken at 154 h (dashed line). Maximal gadusol and biomass measurements for the 2XLys treatments were taken at 131 h (dashed line). Error bars are standard deviations.

The culture treated with 2XLys + 2XTrp (Fig. 17), where the concentration of lysine and tryptophan were doubled, did not grow significantly faster than the 2XTrp or 2XLys treatments (2.1 vs 2.5 vs 2.3 h). The 2XTrp + 2XLys treatment resulted in the largest increase in biomass followed by 2XTrp then 2XLys (A_{600}=5.5>5.0>3.5).

Doubling the concentration of lysine alone had no effect on peak A_{600} (3.5 vs 3.5) or gadusol levels, however it was found to reduce the time to reach final gadusol by 38 h compared to the standard YNB + 2% glucose + lys + trp medium (Fig. 17). Doubling the tryptophan concentration significantly increased biomass, indicating that tryptophan was a limiting nutrient for growth but not gadusol production (Fig. 17). When lysine was doubled in conjunction with tryptophan, biomass increased even further suggesting that lysine was the next nutrient to become growth limiting (Fig. 17). Despite increases in biomass, gadusol levels did not increase significantly. It is unclear why gadusol production did not increase with biomass in the supplemented cultures. I surmise that if accumulated intracellular metabolites inhibited gadusol yield then production should scale proportionally with biomass, which was not observed. Alternatively, inhibition by gadusol or another extracellular metabolite could lead to production that did not scale proportionately and stopped at a certain threshold.

3.6 Deletion of *PHO13* decreases gadusol production

PHO13 encodes a phosphatase whose deletion was found to upregulate the second and third steps of the PPP, 6-phosphogluconolactonase (*SOL3*) and 6-phosphogluconate dehydrogenase (*GND1*) (Kim et al. 2015). *pho13Δ*'s upregulation of

the PPP was originally identified during a screen for mutants with enhanced xylose fermentation rates (Ni et al. 2007). I rationalized that a *pho13Δ* mutation would enhance gadusol yield by increasing expression of two enzymes that provide precursors for S7P biosynthesis. A *pho13Δ* mutant in the *tal1Δ,* gadusol-producing background was designated G9 (Fig. 18).

G9 produced 36% less gadusol (14 vs 22 mg/L) than G1, but required 185.6 h to reach this concentration. In contrast, G1 reached 22 mg/L by 110 h. G9 and G1 reached comparable cell densities (A_{600}=1.6 vs 1.4). G9 grew at the same rate as G1 (t_d=3.6 h). It is unclear why *pho13Δ* lead to a substantial decrease in gadusol yield. Increased expression of the two steps after glucose 6-P dehydrogenase was expected to cause accumulation of PPP intermediates. However, if such accumulation occurred it did not result in improved gadusol yield and hindered production.

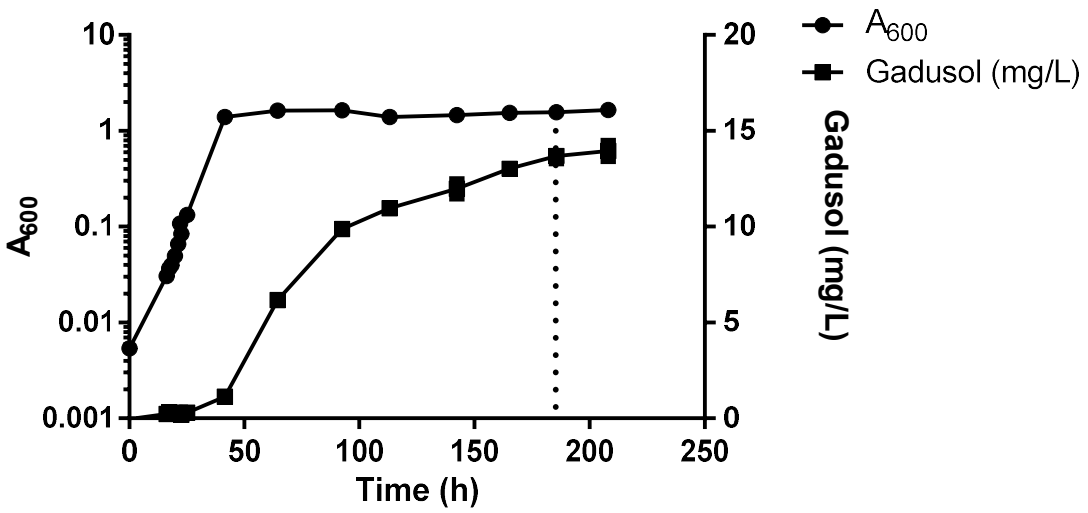

Figure 18. Growth and gadusol production by G9 (*tal1Δ pho13Δ*). Maximal gadusol and biomass measurements for G9 were taken at 186 h (dashed line). Error bars are standard deviations.

3.7 The *SHB17* shunt is a key source of S7P for gadusol biosynthesis

Sedoheptulose 7-P can be generated from the PPP and glycolytic intermediates erythrose 4-P and DHAP by a two-step pathway. Erythrose 4-P and DHAP combine to form sedoheptulose 1,7-P via an additional activity of Fba1 (Clasquin et al. 2011). Sedoheptulose 1,7-P is then dephosphorylated by the phosphatase Shb17 to generate S7P. *SHB17* was deleted to determine if the *SHB17* shunt is a significant source of S7P.

As shown in Figure 19, G6 (*tal1Δ nqm1Δ shb17Δ*) produced 40% less gadusol than G2 (18 mg/L vs 30 mg/L). The G6 strain showed increased biomass production

(A_{600}=2.9 vs 1.4) but grew more slowly (t_d=5.9 vs 3.6 h) than G2. These results show that *SHB17* has a role in generating S7P precursor for gadusol production however the increase in biomass was unexpected. Clasquin et al. (2011) speculated that Shb17 provided a route to generate ribose 5-P precursors without generating NADPH. Based on that hypothesis deletion of *SHB17* should have decreased rather than increased biomass.

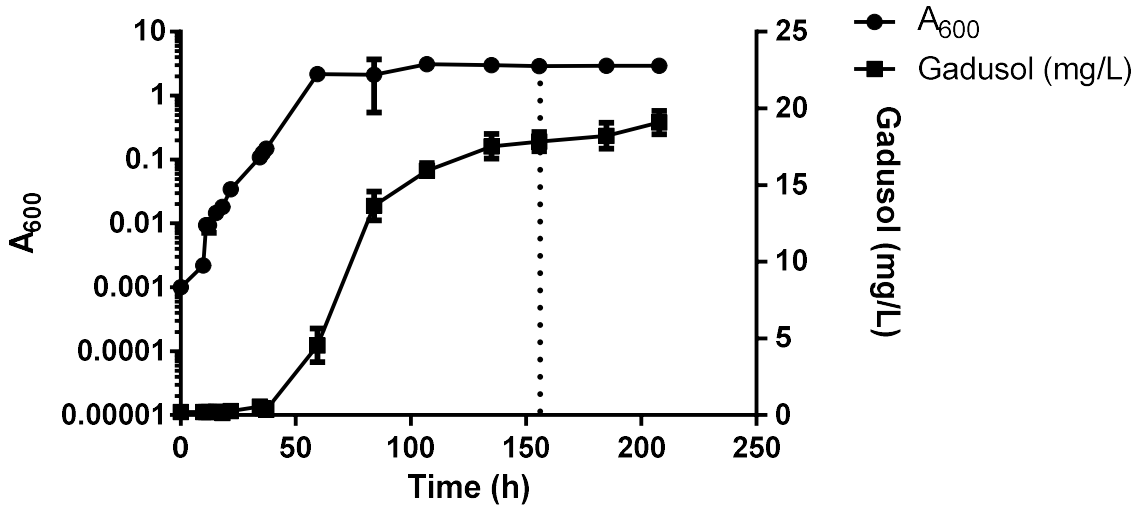

Figure 19. Growth and gadusol production by G6 (*tal1Δ shb17Δ*). Maximal gadusol and biomass measurements for G6 were taken at 156 h (dashed line). Error bars are standard deviations.

3.8 Overexpression of *SHB17* does not increase gadusol yield

Because deletion of *SHB17* reduced gadusol yield, I rationalized that overexpressing *SHB17* would lead to an increase. *SHB17* was overexpressed in the transaldolase mutant strain G3 (*tal1Δ nqm1Δ*) and designated G7. Contrary to expectations, overexpression of *SHB17* decreased gadusol production as shown in Figure 20. G7 produced much less gadusol than G3 (18 vs 64 mg/L). Overexpression of *SHB17* increased biomass (A_{600}=4.8 vs 3.5) and slowed growth (t_d=4.4 vs 1.7 h) compared to G3. These results indicate that overexpression of *SHB17* led to more biomass but reduced gadusol production. Based on these results I speculate that overexpression of *SHB17* may have titrated transcription proteins as described earlier or that accumulation of EEV in the gadusol biosynthesis pathway inhibited production.

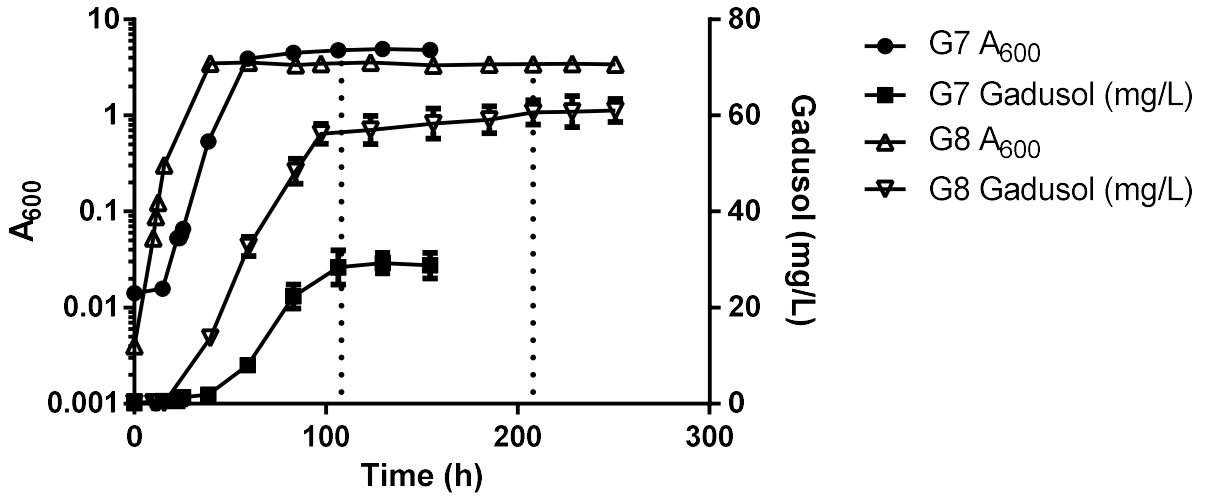

Figure 20. Growth and gadusol production by G7 (*tal1Δ nqm1Δ his3Δ1*::pGH420-EEVS-MTOx/pXP416-SHB17) and G8 (*tal1Δ nqm1Δ his3Δ1*::pGH420-EEVS-MTOx pXP416-SHB17 integrant). Maximal gadusol and biomass measurements for G7 and G8 were taken at 208 and 106 h, respectively (dashed lines). Error bars are standard deviations.

It is unclear why overexpression of *SHB17* failed to increase gadusol yield. Based on the improvement in gadusol production observed when the gadusol construct was integrated I decided to integrate the *SHB17* construct to determine if eliminating plasmid burden would improve yield. The resultant strain was designated G8.

As shown in Figure 20, the G8 strain did not have improved gadusol production (61 vs 64 mg/L) compared to G3. However, it made twice as much gadusol as the G7 strain, which relied on a high-copy plasmid to overexpress *SHB17*. G8 reached a similar biomass (A_{600}=3.4 vs 3.5) to G3 but grew significantly more slowly (t_d=2.0 vs 1.7 h). The restoration of 95% of the gadusol yield by integrating the *SHB17* construct suggests that use of high-copy plasmids inhibits gadusol yield. I speculate that the similar gadusol

yields between G8 and G3 were caused by inhibition at a step after S7P, either the 2-epi-5-epi valiolone synthase or methyl transferase-oxidoreductase steps in gadusol biosynthesis.

3.9 Supplementation with nutrients to increase activity of *SHB17* does not increase gadusol yield

Previous work has shown that growing yeast in YNB + 2% glucose medium with nutrients that require NADPH for biosynthesis increased production of ribose 5-P via the *SHB17* shunt while repressing the PPP reactions that generate NADPH (Clasquin et al. 2011). Supplementing the growth medium for G3 was rationalized to increase gadusol yield by forcing more glycolytic intermediates to enter the PPP via the *SHB17* shunt and increase the amount of available S7P. Supplementation was expected to reduce the requirement for NADPH while maintaining the need for ribose 5-P. Biosynthetic requirements for ribose 5-P were expected to draw intermediates from the *SHB17* shunt towards S7P, providing a source of precursor for gadusol biosynthesis.

As shown in Figure 21, the YNB + NADPH nutr. did not increase gadusol production (68 mg/L vs 64 mg/L) or change biomass (A_{600}=3.8 vs 3.5) of G3. The YNB + NADPH nutr. medium made G3 grow slower than normal (t_d=2.57 vs 1.65 h). The supplementation also increased the time to reach maximal gadusol levels by 61 h (Fig. 21). As I speculated with *SHB17* overexpression, increased availability of S7P may be insufficient to increase gadusol yield if production is inhibited at one of the steps after S7P in gadusol biosynthesis.

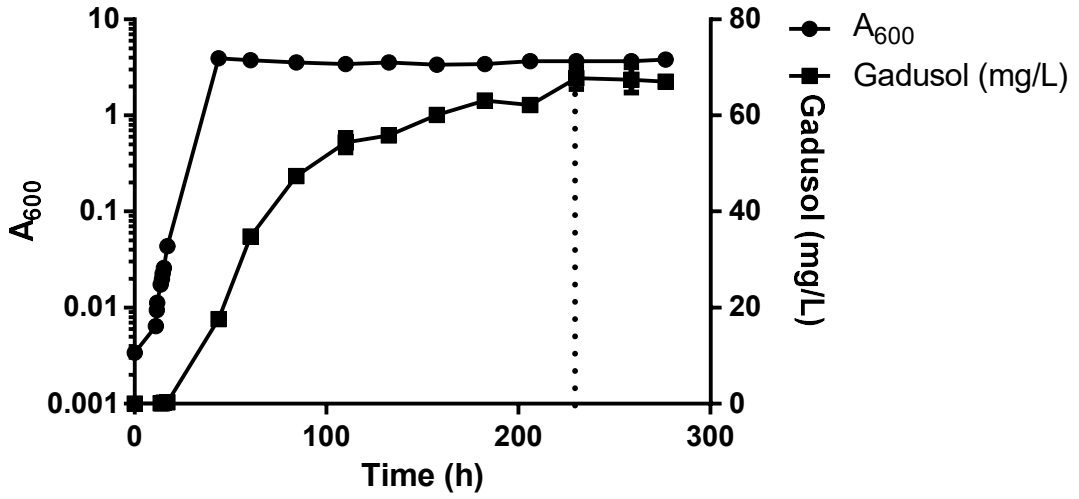

Figure 21. Growth and gadusol production by G3 (*tal1Δ nqm1Δ his3Δ1*::pGH420-EEVS-MTOx) in YNB+NADPH nutr. Maximal gadusol and biomass measurements for G3 grown in YNB+NADPH nutr. were taken at 230 h (dashed line). Error bars are standard deviations.

3.10 Eliminating phosphoglucoisomerase activity in transaldolase mutants does not increase gadusol yield.

Deletion of *PGI1* was rationalized to increase gadusol yields in the transaldolase mutant background based on a report showing a *tal1Δ pgi1Δ* mutant accumulating up to 4-fold more S7P than a *tal1Δ* strain (Schaaff et al. 1990). *PGI1* encodes a phosphoglucoisomerase that converts glucose 6-P to fructose 6-P. Phosphoglucoisomerase-transaldolase double mutants (*pgi1Δ tal1Δ)* are unable to grow on glucose as the sole carbon source because glycolysis is interrupted after glucose 6-P formation (Aguilera 1986). These mutants must rely on the *SHB17* shunt to generate S7P and ribose 5-P. *PGI1* mutants in both the *tal1Δ nqm1Δ* (G4) and *tal1Δ* (G5)

backgrounds were generated. Gadusol production was evaluated in YNB + 2% fructose + 0.1% glucose medium supplemented with lysine for G4 and both lysine and tryptophan for G5.

As shown in Figure 22, eliminating phosphoglucoisomerase activity significantly reduced gadusol production in both G4 and G5. G4 produced much more gadusol than G5 (53 vs 15 mg/L) and reached a higher biomass (A_{600}= 2.6 vs 0.9). However, G4 grew more slowly than G5 (t_d=8.6 vs 4.2 h). The higher gadusol yield by G4 compared to G5 was consistent with observations by Michel et al. (2015) who showed that expression of the second transaldolase Nqm1 increased under glucose-restricted conditions (<0.5%) in *tal1Δ* mutants. G4 and G5 were grown on medium containing 2% fructose and 0.1% glucose, which may have caused upregulation of *NQM1* and concomitant loss of S7P by transaldolase activity in the G5 strain. The absence of transaldolase activity in G4 may have also decreased throughput in the PPP, resulting in elevated levels of ribose 5-P that could translate to greater biomass compared to G5. It is difficult to disentangle the effect *pgi1Δ* had on growth from its effect on gadusol production. G4 produced significantly less gadusol than G3 (53 vs 64 mg/L) and grew much more slowly (t_d=8.6 vs 1.7 h). G4 also reached a lower biomass than G3 (A_{600}=2.6 vs 3.5). I suspect that in addition to the growth defects caused by *pgi1*Δ both G4 and G5 would encounter the same problem that prevented *SHB17* overexpression from increasing gadusol yield. Both interventions were intended to make S7P rate limiting for production of ribose 5-P and presumably biomass. However, gadusol yield either

decreased or was unaffected, suggesting that the step limiting production comes after S7P.

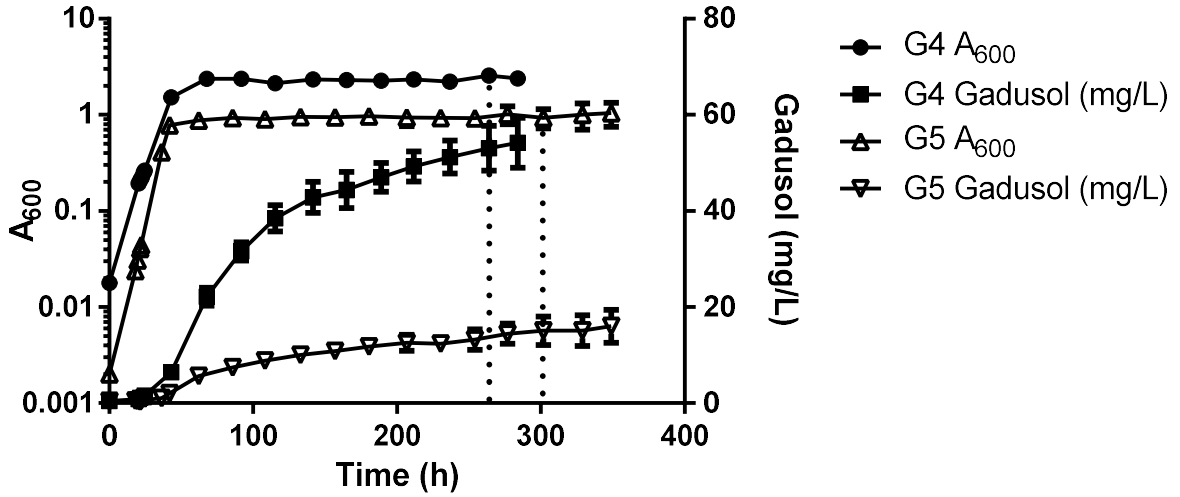

Figure 22. Growth and gadusol production by G4 (*tal1Δ nqm1Δ pgi1Δ*) and G5 (*tal1Δ pgi1Δ*). Maximal gadusol and biomass measurements for G4 and G5 were taken at 264 and 302 h, respectively (dashed lines). Error bars are standard deviations.

3.11 Promoter titration may inhibit gadusol production

Simultaneous integration of the gadusol biosynthesis genes into a yeast chromosome XV and promoter swapping led to a doubling in gadsuol yield from 30 to 64 mg/L. Although the integrated construct used a different promoter for MTOx (P_{PGK1}), this change is unlikely to explain the increase in gadusol yield because P_{PGK1} possess roughly half of the activity of P_{TEF1} as estimated using a GFP assay (Sun et al. 2012).

Promoters on high-copy plasmids can deplete transcription factors, and RNA polymerase activity leading to competition for transcription machinery that is normally in excess. Because constitutive promoters typically come from genes encoding essential processes like translation or glycolysis, promoter titration can lead to growth defects (Görgens et al. 2001). Integration of EEVS and MTOx decreased the doubling time of G3 compared to G2 (t_d=1.7 vs 3.5 h). Integrating EEVS and MTOx would leave limited copies of the promoters in each cell, reducing competition for transcription factors. Using the same promoter (P_{TEF1}) to express both EEVS and MTOx in G2 could have led to reduced expression of these genes in addition to growth defects. Determining expression levels for EEVS and MTOx in the G2 and G3 strains would help determine if gene expression increased after integration or if gadusol yield improved because of changes in growth from plasmid integration.

Observations from the *SHB17* overexpression experiments support a role for promoter titration in gadusol production. Introduction of the high-copy plasmid pXP416-*SHB17* (P_{TEF1}) into the G3 strain led to a sharp decrease in gadusol production (64 vs 28 mg/L). Integration of a construct derived from pXP416-*SHB17* resulted in the near complete restoration of gadusol production in strain G8 (60 vs 64 mg/L). This difference suggests that high-copy plasmids have an inhibitory effect on gadusol production that should be recognized when testing further interventions. Measuring gadusol production and expression of EEVS and MTOx in G3 derivative strains carrying empty P_{TEF1}-expression vector or integrated P_{TEF1}-expression vector would help support this conclusion.

4 Conclusion

This study demonstrated that rational genetic interventions were able to increase gadusol yields approximately 5-fold. Deleting both transaldolase genes (*TAL1* and *NQM1*) resulted in a 2.5-fold increase in gadusol yield compared to the *tal1Δ* mutant. Overexpressing the glucose 6-P dehydrogenase gene (*ZWF1*) in a *tal1Δ* strain caused a 64% increase in gadusol yield. Integrating the gadusol genes and switching the promoter for MTOx doubled gadsuol production relative to a *tal1Δ nqm1Δ* strain expressing the gadusol genes from free plasmids. In most of the strains studied, 83-98% of gadusol was made after exiting log phase.

5 References

Aguilera A (1987) Mutations suppressing the effects of a deletion of the Phosphoglucose isomerase gene PGI1 in *Saccharomyces cerevisiae*. Curr Genet 11:429–434. doi: 10.1007/BF00384603

Aguilera A (1986) Deletion of the phosphoglucose isomerase structural gene makes growth and sporulation glucose dependent in *Saccharomyces cerevisiae*. Mol Gen Genet 204:310–316

Arbeloa EM, Bertolotti SG, Churio MS (2011) Photophysics and reductive quenching reactivity of gadusol in solution. Photochem Photobiol Sci 10:133–42. doi: 10.1039/c0pp00250j

Arbeloa EM, Uez MJ, Bertolotti SG, Churio MS (2010) Antioxidant activity of gadusol and occurrence in fish roes from Argentine Sea. Food Chem 119:586–591. doi: 10.1016/j.foodchem.2009.06.061

Baudin A, Ozier-kalogeropoulos O, Denouel A, et al (1993) A simple and efficient method for direct gene deletion in *Saccharomyces cerevisiae*. Nucleic Acids Res 21:3329–3330. doi: 10.1093/nar/21.14.3329

Bok MJ, Porter ML, Place AR, Cronin TW (2014) Biological Sunscreens Tune Polychromatic Ultraviolet Vision in Mantis Shrimp. Curr Biol 24:1636–1642. doi: 10.1016/j.cub.2014.05.071

Booth C, Morrow J (1997) The penetration of UV into natural waters. Photochem Photobiol 65:355–358

Cadière A, Ortiz-Julien A, Camarasa C, Dequin S (2011) Evolutionary engineered *Saccharomyces cerevisiae* wine yeast strains with increased in vivo flux through the pentose phosphate pathway. Metab Eng 13:263–271. doi: 10.1016/j.ymben.2011.01.008

Chioccara F, Zeuli L, Novellino E (1986) Occurrence of mycosporine related compounds in sea urchin eggs. Comp Biochem Physiol 85:459–461. doi: 10.1016/0305-0491(86)90027-1

Clasquin MF, Melamud E, Singer A, et al (2011) Riboneogenesis in yeast. Cell 145:969–980. doi: 10.1016/j.cell.2011.05.022

Ding J, Holzwarth G, Bradford CS, et al (2015) PEP3 overexpression shortens lag phase but does not alter growth rate in *Saccharomyces cerevisiae* exposed to acetic acid stress. Appl Microb Cell Physiol 99:8667–8680. doi: 10.1007/s00253-015-6708-9

Dunlap WC, Williams DM, Chalker BE, Banaszak AT (1989) Biochemical protoadaption in vision: UV absorbing pigments in fish eye tissue. Comp Biochem Physiol 93B:601–607

Fang F, Salmon K, Shen MWY, et al (2011) A vector set for systematic metabolic engineering in *Saccharomyces cerevisiae*. Yeast 3:123–136. doi: 10.1002/yea

Gao Q, Garcia-Pichel F (2011) Microbial ultraviolet sunscreens. Nat Rev Microbiol 9:791–802. doi: 10.1038/nrmicro2649

Garcia-Pichel F (1998) Solar ultraviolet and the evolutionary history of cyanobacteria. In: Origins of Life and Evolution of the Biosphere. pp 321–347

Garcia-Pichel F (1994) A model for internal self-shading in planktonic organisms and its implications for the usefulness of ultraviolet sunscreens. Limnol Oceanogr 39:1704–1717. doi: 10.4319/lo.1994.39.7.1704

Gietz RD, Woods R (2001) Genetic transformation of yeast. Biotechniques 30:816–831

Görgens JF, Van Zyl WH, Knoetze JH, Hahn-Hägerdal B (2001) The metabolic burden of the PGK1 and ADH2 promoter systems for heterologous xylanase production by *Saccharomyces cerevisiae* in defined medium. Biotechnol Bioeng 73:238–245. doi: 10.1002/bit.1056

Grabowska D, Chelstowska A (2003) The ALD6 gene product is indispensable for providing NADPH in yeast cells lacking glucose-6-phosphate dehydrogenase activity. J Biol Chem 278:13984–8. doi: 10.1074/jbc.M210076200

Grant PT (1980) Gadusol, a metabolite from fish eggs. Tetrahedron Lett 21:4043–4044

Huang H, Rong H, Li X, et al (2008) The crystal structure and identification of NQM1/YGR043C, a transaldolase from *Saccharomyces cerevisiae*. Proteins Struct Funct Bioinforma 73:1076–1081. doi: 10.1002/prot.22237

Kim SR, Xu H, Lesmana A, et al (2015) Deletion of PHO13, Encoding Haloacid Dehalogenase Type IIA Phosphatase, Results in Upregulation of the Pentose Phosphate Pathway in *Saccharomyces cerevisiae*. Appl Environ Microbiol 81:1601–1609. doi: 10.1128/AEM.03474-14

Kuijpers NGA, Solis-escalante D, Bosman L, et al (2013) A versatile, efficient strategy for assembly of multi-fragment expression vectors in *Saccharomyces cerevisiae* using 60 bp synthetic recombination sequences. Microb Cell Fact 12:1–13

Michel S, Keller MA, Wamelink MMC, Ralser M (2015) A haploproficient interaction of the transaldolase paralogue NQM1 with the transcription factor VHR1 affects stationary phase survival and oxidative stress resistance. BMC Genet 16:13. doi: 10.1186/s12863-015-0171-6

Minard KI, McAlister-Henn L (2005) Sources of NADPH in yeast vary with carbon source. J Biol Chem 280:39890–39896. doi: 10.1074/jbc.M509461200

Ng CH, Tan SX, Perrone GG, et al (2008) Adaptation to hydrogen peroxide in *Saccharomyces cerevisiae*: The role of NADPH-generating systems and the SKN7 transcription factor. Free Radic Biol Med 44:1131–1145. doi: 10.1016/j.freeradbiomed.2007.12.008

Ni H, Laplaza JM, Jeffries TW (2007) Transposon mutagenesis to improve the growth of recombinant *Saccharomyces cerevisiae* on D-xylose. Appl Environ Microbiol 73:2061–2066. doi: 10.1128/AEM.02564-06

Osborn AR, Almabruk KH, Holzwarth G, et al (2015) De novo synthesis of a sunscreen compound in vertebrates. Elife 4:1–15. doi: 10.7554/eLife.05919

Pernambuco MB, Winderickx J, Crauwels M, et al (1996) Glucose-triggered signaling in *Saccharomyces cerevisiae*: different requirements for sugar phosphorylation between cells grown on non-fermentable carbon sources. Microbiology 142:1775–1782. doi: 10.1099/13500872-142-7-1775

Plack PA, Fraser NW, Grant PT, et al (1981) Gadusol, an enolic derivative of cyclohexane-1,3-dione present in the roes of cod and other marine fish. Biochem J 199:741–747

Ralser M, Wamelink MM, Kowald A, et al (2007) Dynamic rerouting of the carbohydrate flux is key to counteracting oxidative stress. J Biol 6:10. doi: 10.1186/jbiol61

Ro DK, Paradise EM, Quellet M, et al (2006) Production of the antimalarial drug precursor artemisinic acid in engineered yeast. Nature 440:940–943. doi: 10.1038/nature04640

Schaaff I, Hohmann S, Zimmermann FK (1990) Molecular analysis of the structural gene for yeast transaldolase. Eur J Biochem 188:597–603. doi: 10.1111/j.1432-1033.1990.tb15440.x

Schwartz K, Sherlock G (2016) Preparation of yeast DNA sequencing libraries. Cold Spring Harb Protoc 2016:871–876. doi: 10.1101/pdb.prot088930

Sinha RP, Häder D-P (2002) UV-induced DNA damage and repair: a review. Photochem Photobiol Sci 1:225–236. doi: 10.1039/b201230h

Stincone A, Prigione A, Cramer T, et al (2015) The return of metabolism: Biochemistry and physiology of the pentose phosphate pathway. Biol Rev 90:927–963. doi: 10.1111/brv.12140

Sun J, Shao Z, Zhao H, et al (2012) Cloning and Characterization of a Panel of Constitutive Promoters for Applications in Pathway Engineering in *Saccharomyces cerevisiae*. 109:2082–2092. doi: 10.1002/bit.24481

Thodey K, Galanie S, Smolke CD (2014) A microbial biomanufacturing platform for natural and semisynthetic opioids. Nat Chem Biol 1–10. doi: 10.1038/nchembio.1613

Van Winden WA, Van Dam JC, Ras C, et al (2005) Metabolic-flux analysis of *Saccharomyces cerevisiae* CEN.PK113-7D based on mass isotopomer measurements of 13C-labeled primary metabolites. FEMS Yeast Res 5:559–568. doi: 10.1016/j.femsyr.2004.10.007

Appendices

6.1 Construction of pGH420-EEVS-MTOx

A plasmid expressing both EEVS and MTOx was constructed using *in vivo* ligation as described, according to the scheme outlined in Fig. 1 (Kuijpers et al, 2013). The essential elements in the construct were synthesized via PCR as seven individual amplicons sharing terminal homology that directed ligation and recombination in a unique order. The seven amplicons are numbered, and the terminal sequence regions are lettered in Fig. 1. For example, sequence A mediates ligation between amplicons 1 and 7 and sequence B mediates ligation between amplicons 1 and 2. The plasmid was designed to place the yeast origin of replication (2μ) and selectable marker (*HIS3*) on non-contiguous amplicons because previous work demonstrated that such a separation reduced the number of false positive transformants (Kuijpers et al. 2013).

PCR primers designed to amplify DNA sequences containing the *HIS3* marker, *PGK1* promoter, MTOx ORF, *PGK1* terminator, 2μ yeast ORI, *E. coli* AMP^r-ORI sequence, and the EEVS expression cassette are listed in appendix 6.2. Primers containing 5'-60-

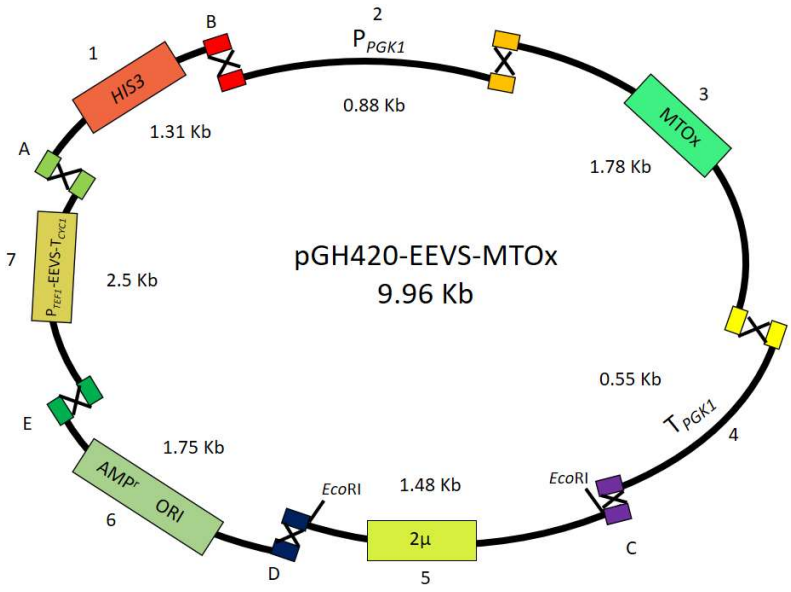

Figure 23. Scheme for constructing pGH420-EEVS-MTOx by *in vivo* ligation.

bp barcode sequences were designed using the sequences described in appendix 6.3. The barcode sequences lacked homology to the yeast genome, limiting the risk of chromosomal recombination. In the case of MTOx (3) a portion of the ORF sequence was used to target recombination. Specifically, the downstream end of fragment 2 contained 60-bp of homology to the 5'-region of the MTOx ORF while the upstream region of fragment 4 contained 60-bp of homology to 3'-region of the MTOx ORF.

The PCR conditions used to amplify the components of the plasmid construct were modified from the manufacturer's instructions for the polymerase (Thermofisher Phusion Hot Start II). Primer concentrations were lowered from 500 to 200 nM and polymerase concentration was raised from 0.02 to 0.03 U/μl. Amplicons were gel-purified using a Qiagen gel purification kit. To improve DNA extraction, after a PCR amplicon was excised from a horizontal gel, the slice was cut into a top layer (A) and a bottom layer (B) (Fig. 24). The bottom layer typically contained most of the DNA and was processed according to the manufacturer's instructions while the top layer (A) was disposed of. Approximately 200 fmol each of the purified 2μ and *HIS3* amplicons and 100 fmol each of the purified MTOx ORF, EEVS cassette, *E. coli* AMP^r-ORI, *PGK1* promoter, and terminator amplicons were used to transform BY4742 *tal1Δ trp1Δ nqm1Δ* using the lithium-acetate method (Gietz and Woods 2001). Transformants were selected and maintained on

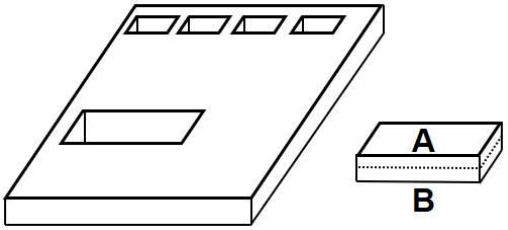

Figure 24. Gel dissection for DNA purification

M+lys+trp plates. Transformants were screened for gadusol production in 1 ml YNB + 2% glucose + lys + trp screwcap-tube cultures shaken at 200 RPM and 30° C for 72-h. A gadusol-producing strain was then screened for the *E. coli* AMP^r-ORI sequence using the primers F-ORI-F/H-AMP-R to generate a 1.8 Kb PCR amplicon. The pGH420-EEVS-MTOx plasmid was extracted using Zymoprep yeast plasmid miniprep II kit (Zymoresearch). A 5-µl aliquot of yeast plasmid DNA was used to transform competent TOP10 *E. coli* cells (Invitrogen). Transformants were selected and maintained on LB+amp plates. Then a transformant was selected for culturing and plasmid DNA purification using a Qiaquick plasmid miniprep kit. Plasmid construction was confirmed by *EcoRI* digestion and analysis by agarose gel electrophoresis, yielding 8.5 and 1.5 Kb fragments.

6.2 Primers used to construct pGH420-EEVS-MTOx

Table 6. Details for primers used to construct pGH420-EEVS-MTOx

Name	Sequence (5′–3′)	Template	PCR product (Kb)	Primer T_m (°C)	Annealing temperature (°C)
A-HIS3-F	ACTATATGTGAAGGCATGGCTATGGCAC GGCAGACATTCCGCCAGATCATCAATAG GCACcttcattcaacgtttcccatt	S288c	1.31	61.6	57.5
B-HIS3-R	GTTGAACATTCTTAGGCTGGTCGAATCAT TTAGACACGGGCATCGTCCTCTCGAAAG GTGtgatgcattaccttgtcatc			57.5	
B-PPGK1-FII	ACCTTTCGAGAGGACGATGCCCGTGTCT AAATGATTCGACCAGCCTAAGAATGTTCA ACcctgacttcaactcaagacgc	S288c	0.88	64.3	64.3
MT-P_{PGK1}-RII	CAGCAGATGTTCCACAATAAATTCAACCG GGGTGTCCGAGACTTTTGCCGTTTGCATa ctagtatatttgttgtaaaaagtagataattacttcc			64.9	
MTOx-F	ACGTCTCACGGATCGTATATGCCGTAGC GACAATCTAAGAACTATGCGAGGACACG CTAGactagtatgcaaacggcaaaagtctc	pXP416-MTOx	1.78	65.2	68.2
MTOx-R	AATCACTCTCCATACAGGGTTTCATACAT TTCTCCACGGGACCCACAGTCGTAGATG CGT ctcgagtcaccacagagactgaccg			71.2	
Ox-T_{PGK1}-FII	GCATCCGACTACATGACCGGTCACAATC TGGTTATTGAAGGCGGTCAGTCTCTGTG GTGA attgaattgaattgaaatcgatagatca	S288c	0.55	65.3	64.5
C-T_{PGK1}-RII	GCCTACGGTTCCCGAAGTATGCTGCTGA TGTCTGGCTATACCTATCCGTCTACGTGA ATAttttgttgcaagtgggatga			64.5	
C-2μ-F	TATTCACGTAGACGGATAGGTATAGCCA GACATCAGCAGCATACTTCGGGAACCGT AGGC gaattcgtatgatccaatatc	pXP416-MTOx	1.48	54.1	57.1
D-2μ-R	TGCCGAACTTTCCCTGTATGAAGCGATCT GACCAATCCTTTGCCGTAGTTTCAACGTA TG gaattcaacgaagcatctgtgc			64.6	
D-ORI-F	CATACGTTGAAACTACGGCAAAGGATTG GTCAGATCGCTTCATACAGGGAAAGTTC GGCAaaaggcggtaatacggtta	pXP416-MTOx	1.75	57.7	55.2
E-AMP-R	GTCACGGGTTCTCAGCAATTCGAGCTATT ACCGATGATGGCTGAGGCGTTAGAGTAA TCTgaaaaaggaagagtatgagtattc			55.2	
E-PTEF1-F	AGATTACTCTAACGCCTCAGCCATCATCG GTAATAGCTCGAATTGCTGAGAACCCGT GAC accgcgaatccttacatcac	pXP420-EEVS	2.5	62.7	62.7
A-TCYC1-RII	GTGCCTATTGATGATCTGGCGGAATGTCT GCCGTGCCATAGCCATGCCTTCACATATA GTcagacaagctgtgaccgtct			62.1	

Upper case sequences provide short flanking homology between PCR products while lower case sequences are homologous to template DNA.

6.3 Barcode sequences to facilitate *in vivo* ligation

Table 7. Barcode sequences

Barcode sequence	Sequence 5'-3'
A	ACTATATGTGAAGGCATGGCTATGGCACGGCAGACATTCCGCCAGATCATCAATAGGCAC
B	CACCTTTCGAGAGGACGATGCCCGTGTCTAAATGATTCGACCAGCCTAAGAATGTTCAAC
C	TATTCACGTAGACGGATAGGTATAGCCAGACATCAGCAGCATACTTCGGGAACCGTAGGC
D	CATACGTTGAAACTACGGCAAAGGATTGGTCAGATCGCTTCATACAGGGAAAGTTCGGCA
E	AGATTACTCTAACGCCTCAGCCATCATCGGTAATAGCTCGAATTGCTGAGAACCCGTGAC

6.4 DNA sequences

6.4.1 EEVS, *E. coli* codon-optimized *D. rerio* ORF (Osborn et al. 2015)

ATGGAACGTCCGGGCGAAACCTTTACCGTCAGCTCCCCGGAAGAAGTGCGTCTGC

CGTCTGTTCACCGCGATAACTCAACGATGGAAAACCATAATAAACAGGAAACGGTG

TTTTCTCTGGTTCAAGTCAAGGGTACCTGGAAGCGTAAGGCGGGCCAGAACGCCA

AACAGGGTATGAAGGGCCGCGTTAGTCCGGCCAAAATTTATGAAAGCTCTAGTTCC

TCAGGTACCACGTGGACGGTGGTTACCCCGATCACCTTTACGTACACCGTGACGC

AGACCAAAAACCTGCTGGACCCGTCGAACGACACGCTGCTGCTGGGCCATATTAT

CGATACCCAGCAACTGGAAGCTGTCCGCAGCAATACGAAACCGCTGAAGCGTTTC

ATTGTGATGGACGAAGTCGTGTATAATATCTACGGTTCCCAAGTCACCGAATATCT

GGAAGCGCGCAACGTGCTGTACCGTATTCTGCCGCTGCCGACCACGGAAGAAAAT

AAATCAATGGATATGGCTCTGAAGATTCTGGAAGAAGTGCACCAGTTTGGTATCGA

CCGTCGCACCGAACCGATTATCGCGATTGGCGGTGGCGTTTGCCTGGATATCGTC

GGTCTGGCAGCCTCTCTGTATCGTCGCCGTACCCCGTACATTCGTGTGCCGACCA

CGCTGCTGTCTTATATCGACGCAAGTGTGGGTGCTAAAACGGGCGTTAACTTTGCT

AATTGTAAAAACAAGCTGGGTACCTACATTGCGCCGGTTGCAGCTTTTCTGGATCG

TTCGTTCATTCAGAGCATCCCGCGCCGTCACATCGCAAACGGTCTGGCCGAAATG

CTGAAAATGGCCCTGATGAAGCATCGCGGTCTGTTCGAACTGCTGGAAGTTCACG
GCCAGTTTCTGCTGGATAGTAAATTCCAATCGGCAAGCGTCCTGGAAAACGATCGC
ATTGACCCGGCCTCTGTCAGTACGCGTGTGGCAATCGAAACCATGCTGGAAGAAC
TGGCCCCGAATCTGTGGGAAGATGACCTGGATCGTCTGGTGGACTTTGGTCATCT
GATTTCGCCGCAGCTGGAAATGAAAGTTCTGCCGGCACTGCTGCACGGCGAAGCT
GTCAACATTGATATGGCGTATATGGTGTACGTTTCATGCGAAATCGGTCTGCTGAC
CGAAGAAGAAAAATTCCGCATTATCTGCTGTATGATGGGCCTGGAACTGCCGGTGT
GGCATCAGGATTTTACCTTCGCACTGGTTCAAAAGTCCCTGTGTGACCGCCTGCAG
CACTCAGGTGGCCTGGTTCGTATGCCGCTGCCGACGGGTCTGGGTCGTGCAGAA
ATTTTTAATGATACCGACGAAGGTAGCCTGTTCCGCGCGTATGAAAAATGGTGCGA
TGAACTGTCCACCGGCTCACCGCAGTGA

6.4.2 MTOx, *E. coli* codon-optimized *D. rerio* ORF (Osborn et al. 2015)

ATGCAAACGGCAAAAGTCTCGGACACCCCGGTTGAATTTATTGTGGAACATCTGCT
GAAGGCTAAGGAAATCGCTGAAAATCACGCTTCCATTCCGGTGGAACTGCGCGAT
AACCTGCAGAAAGCTCTGGATATCGCGAGCGGCCTGGACGAATATCTGGAACAAA
TGAGCTCTAAAGAATCTGAACCGCTGACGGAACTGTACCGCAAGTCAGTCTCGCAT
GATTGGAATAAAGTGCACGCGGACGGCAAGACCCTGTTTCGTCTGCCGGTGACCT
GCATTACGGGCCAGGTCGAAGGTCAAGTGCTGAAAATGCTGGTTCACATGAGTAA
AGCGAAGCGTGTCCTGGAAATTGGCATGTTTACCGGCTATGGTGCCCTGTCCATG
GCAGAAGCTCTGCCGGAAAACGGTCAGCTGATCGCTTGTGAACTGGAACCGTACC
TGAAAGATTTTGCACAACCGATTTTCGACAAGAGTCCGCATGGCAAAAAGATCACC

GTGAAAACGGGTCCGGCAATGGATACCCTGAAGGAACTGGCGGCCACGGGCGAA

CAGTTTGACATGGTTTTCATTGATGCGGACAAGCAAAACTACATCAACTACTACAAG

TTCCTGCTGGATCACAACCTGCTGCGTATTGATGGCGTCATCTGCGTGGACAATAC

GCTGTTCAAAGGTCGCGTGTACCTGAAGGATAGCGTTGACGAAATGGGTAAAGCC

CTGCGTGATTTTAACCAGTTCGTGACCGCAGACCCGCGTGTTGAACAAGTCATTAT

CCCGCTGCGCGATGGCCTGACCATTATCCGTCGCGTCCCGTATACGCCGCAGCC

GAATAGCCAATCTGGTACCGTGACGTACGATGAAGTTTTTCGCGGCGTCCAGGGT

AAACCGGTTCTGGATCGTCTGCGCCTGGACGGCAAAGTGGCTTATGTTACCGGTG

CCGGTCAGGGTATTGGTCGTGCATTCGCCCATGCACTGGGCGAAGCTGGTGCGAA

AGTTGCCATTATCGATATGGACCGTGGCAAGGCCGAAGATGTCGCACACGAACTG

ACCCTGAAAGGTATTAGTTCCATGGCCGTGGTTGCAGATATCAGCAAACCGGATGA

CGTGCAGAAGATGATTGATGACATCGTTACCAAATGGGGCACGCTGCATATTGCTT

GCAACAATGCGGGTATCAACAAAAATAGTGCGTCCGAAGAAACCTCTCTGGAAGAA

TGGGATCAGACGTTTAACGTCAATCTGCGTGGCACCTTCATGTGCTGTCAGGCAG

CTGGTCGCGTTATGCTGAAACAAGGCTATGGCAAGATTATCAACACCGCTAGCATG

GCGTCTCTGATTGTGCCGCACCCGCAGAAACAACTGTCATACAATACGTCGAAAG

CCGGCGTCGTGAAGCTGACCCAGACGCTGGGCACCGAATGGATCGATCGTGGTG

TGCGCGTTAACTGTATTTCACCGGGTATCGTGGATACCCCGCTGATTCATTCAGAA

TCGCTGGAACCGCTGGTTCAGCGTTGGCTGTCGGATATCCCGGCAGGTCGTCTGG

CACAGGTGACGGACCTGCAAGCGGCCGTTGTCTATCTGGCCAGTGATGCATCCGA

CTACATGACCGGTCACAATCTGGTTATTGAAGGCGGTCAGTCTCTGTGGTGA

6.4.3 *SHB17*, sedoheptulose 1,7-bisphosphatase ORF from *S. cerevisiae* (Clasquin et al. 2011)

ATGCCTTCGCTAACCCCCAGATGTATCATTGTCAGACACGGTCAAACTGAATGGTC

CAAGTCAGGCCAGTATACTGGTTTGACAGATCTACCGTTAACGCCCTACGGTGAG

GGCCAAATGTTGAGGACCGGTGAGAGTGTTTTCCGCAATAATCAGTTTTTGAATCC

AGACAACATCACTTATATCTTCACCTCTCCACGTTTGCGTGCCAGGCAAACTGTGG

ATTTGGTTTTGAAACCATTAAGCGACGAGCAAAGAGCTAAGATCCGTGTGGTGGTA

GACGACGACTTGCGAGAGTGGGAGTACGGTGACTACGAGGGAATGCTGACTCGA

GAAATCATTGAATTGAGAAAGTCACGCGGTTTGGACAAGGAGAGGCCATGGAATAT

CTGGAGAGATGGGTGTGAGAACGGTGAGACTACTCAGCAAATTGGGTTGAGACTT

TCCCGCGCTATTGCCAGAATCCAGAACTTGCACCGCAAGCACCAGAGTGAGGGCA

GAGCATCAGACATCATGGTCTTTGCGCACGGACATGCATTGCGTTATTTTGCTGCT

ATTTGGTTTGGACTGGGTGTGCAAAAGAAGTGTGAGACGATTGAAGAAATTCAAAA

TGTCAAATCTTATGATGACGACACAGTTCCATATGTGAAATTGGAATCTTACAGACA

TTTGGTAGACAATCCATGTTTCTTACTGGACGCCGGTGGGATTGGTGTTTTGTCAT

ACGCTCACCACAACATTGACGAACCTGCATTGGAATTAGCAGGTCCATTTGTCTCA

CCACCAGAGGAGGAATCCCAGCATGGCGATGTGTAA

6.4.4 *ZWF1*, glucose 6-P dehydrogenase ORF from *S. cerevisiae* (Schaaff et al. 1990)

ATGAGTGAAGGCCCCGTCAAATTCGAAAAAAATACCGTCATATCTGTCTTTGGTGC

GTCAGGTGATCTGGCAAAGAAGAAGACTTTTCCCGCCTTATTTGGGCTTTTCAGAG

AAGGTTACCTTGATCCATCTACCAAGATCTTCGGTTATGCCCGGTCCAAATTGTCC

ATGGAGGAGGACCTGAAGTCCCGTGTCCTACCCCACTTGAAAAAACCTCACGGTG

AAGCCGATGACTCTAAGGTCGAACAGTTCTTCAAGATGGTCAGCTACATTTCGGGA

AATTACGACACAGATGAAGGCTTCGACGAATTAAGAACGCAGATCGAGAAATTCGA

GAAAAGTGCCAACGTCGATGTCCCACACCGTCTCTTCTATCTGGCCTTGCCGCCA

GCGTTTTTTTGACGGTGGCCAAGCAGATCAAGAGTCGTGTGTACGCAGAGAATGG

CATCACCCGTGTAATCGTAGAGAAACCTTTCGGCCACGACCTGGCCTCTGCCAGG

GAGCTGCAAAAAAACCTGGGGCCCCTCTTTAAAGAAGAAGAGTTGTACAGAATTGA

CCATTACTTGGGTAAAGAGTTGGTCAAGAATCTTTTAGTCTTGAGGTTCGGTAACCA

GTTTTTGAATGCCTCGTGGAATAGAGACAACATTCAAAGCGTTCAGATTTCGTTTAA

AGAGAGGTTCGGCACCGAAGGCCGTGGCGGCTATTTCGACTCTATAGGCATAATC

AGAGACGTGATGCAGAACCATCTGTTACAAATCATGACTCTCTTGACTATGGAAAG

ACCGGTGTCTTTTGACCCGGAATCTATTCGTGACGAAAAGGTTAAGGTTCTAAAGG

CCGTGGCCCCCATCGACACGGACGACGTCCTCTTGGGCCAGTACGGTAAATCTGA

GGACGGGTCTAAGCCCGCCTACGTGGATGATGACACTGTAGACAAGGACTCTAAA

TGTGTCACTTTTGCAGCAATGACTTTCAACATCGAAAACGAGCGTTGGGAGGGCGT

CCCCATCATGATGCGTGCCGGTAAGGCTTTGAATGAGTCCAAGGTGGAGATCAGA

CTGCAGTACAAAGCGGTCGCATCGGGTGTCTTCAAAGACATTCCAAATAACGAACT

GGTCATCAGAGTGCAGCCCGATGCCGCTGTGTACCTAAAGTTTAATGCTAAGACC

CCTGGTCTGTCAAATGCTACCCAAGTCACAGATCTGAATCTAACTTACGCAAGCAG

GTACCAAGACTTTTGGATTCCAGAGGCTTACGAGGTGTTGATAAGAGACGCCCTAC

TGGGTGACCATTCCAACTTTGTCAGAGATGACGAATTGGATATCAGTTGGGGCATA

TTCACCCCATTACTGAAGCACATAGAGCGTCCGGACGGTCCAACACCGGAAATTTA

CCCCTACGGATCAAGAGGTCCAAAGGGATTGAAGGAATATATGCAAAAACACAAGT

ATGTTATGCCCGAAAAGCACCCTTACGCTTGGCCCGTGACTAAGCCAGAAGATAC

GAAGGATAATTAG

6.5 Estimating exit from log phase

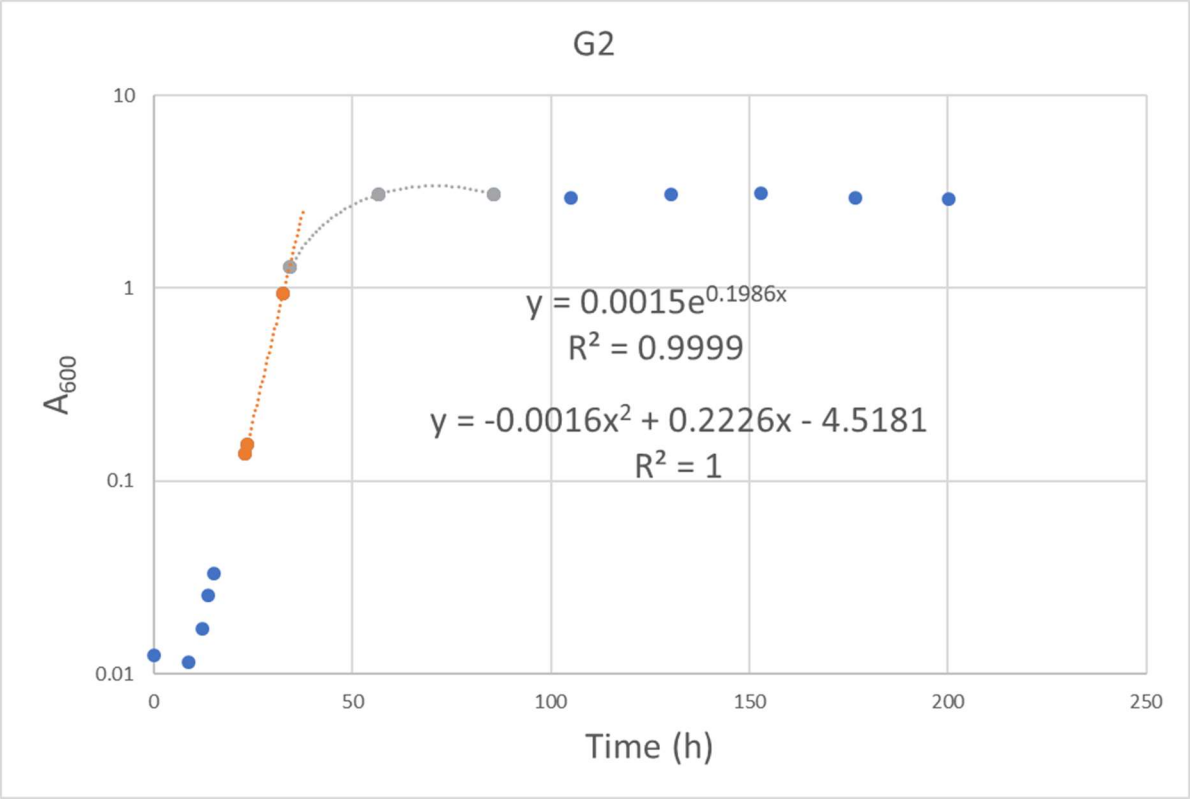

Figure 25. Determining exit from log phase for G2.

Figure 25. provides an example of how exit from log phase was determined for the strains using G2. The exponentialgrowth equation $0.0015e^{0.1986x}$ was generated by fitting a trend line to G2 cultures growing exponentially. The polynomial trend line equation $-0.0016x^2+0.2226x-4.5181$ was generated by fitting a trend line to G2 cultures exiting log phase. Exit from log phase was determined by solving for the intersection of the exponential growth and polynomial trend lines.